

**İSTANBUL TECHNICAL UNIVERSITY ★ INSTITUTE OF SCIENCE AND TECHNOLOGY**

**RELIABILITY AND SECURITY OF  
ARBITER BASED PHYSICAL UNCLONABLE FUNCTION**

**M.Sc. Thesis by  
Zaur TARIGULIYEV**

**Department : Electronics and Communication Engineering**

**Programme : Electronics Engineering**

**JANUARY 2011**



**RELIABILITY AND SECURITY OF  
ARBITER BASED PHYSICAL UNCLONABLE FUNCTION**

**M.Sc. Thesis by  
Zaur TARIGULIYEV  
504021229**

**Date of submission : 20 December 2010  
Date of defence examination : 25 January 2011**

**Supervisor (Chairman) : Assis. Prof. Dr. Siddika Berna ORS YALCİN (ITU)  
Members of the Examining Committee : Prof. Dr. Ece Olcay GUNES (ITU)  
Assis. Prof. Dr. Gökay SALDAMLI (BU)**

**JANUARY 2011**



**İSTANBUL TEKNİK ÜNİVERSİTESİ ★ FEN BİLİMLERİ ENSTİTÜSÜ**

**FLİP-FLOP TABANLI FİZİKSEL KOPYALANAMAZ FONKSİYONUN  
GÜVENLİĞİ VE GÜVENİRLİĞİ**

**YÜKSEK LİSANS TEZİ  
Zaur TARIGULİYEV  
504021229**

**Tezin Enstitüye Verildiği Tarih : 20 Aralık 2010**

**Tezin Savunulduğu Tarih : 25 Ocak 2011**

**Tez Danışmanı : Yrd. Doç. Dr. Sıddıka Berna ÖRS YALÇIN (İTÜ)  
Diğer Jüri Üyeleri : Prof. Dr. Ece Olcay GÜNEŞ (İTÜ)  
Yrd. Doç. Dr. Gökay SALDAMLI (BÜ)**

**OCAK 2011**



## **FOREWORD**

I would like to extend my sincere gratitude to my advisor, Berna ÖRS, for her inspiring advice and encouragement through the beginning to the end of this search. I would like to express my appreciation and thanks to Zafer Işcan, my best friend, for giving me the PR software tool, and help with translation from english to turkish. Furthermore, I'm thankful to my friends from Embedded System laboratory for technical support in experiments with the FPGA.

December 2010

Zaur TARIGULIYEV

Electronics Engineer



## TABLE OF CONTENTS

	<u>Page</u>
<b>TABLE OF CONTENTS</b> .....	<b>vii</b>
<b>ABBREVIATIONS</b> .....	<b>ix</b>
<b>LIST OF TABLES</b> .....	<b>xi</b>
<b>LIST OF FIGURES</b> .....	<b>xiii</b>
<b>SUMMARY</b> .....	<b>xv</b>
<b>ÖZET</b> .....	<b>xvii</b>
<b>1. INTRODUCTON</b> .....	<b>1</b>
<b>2. DEFINITION AND APPLICATION OF PHYSICAL UNCLONABLE FUNCTIONS</b> .....	<b>5</b>
2.1 Definition of One–Way Function.....	5
2.2 Definition of a Physical Unclonable Function.....	6
2.3 PUF Based RFID Authentication.....	7
<b>3. DESCRIPTION AND LINEER MODEL OF PUF CIRCUIT</b> .....	<b>9</b>
3.1 General Description.....	9
3.2 Components of PUF Circuit.....	10
3.3 Delay Paths in the PUF Circuit .....	12
3.3.1 Switch delay .....	12
3.3.2 Delay path configurations .....	13
3.4 Symmetrical Structure of PUF circuit .....	15
3.5 Lineer Model of an Arbiter-based PUF.....	17
<b>4. IMPLEMENTATION OF A PHYSICAL UNCLONABLE FUNCTION ON THE FPGA</b> .....	<b>21</b>
4.1 Introduction to an FPGA .....	21
4.2 Implementation of PUF components.....	22
4.2.1 Switch implemented with MUX.....	22
4.2.2 The Arbiter .....	25
4.3 Placement of Switch Box.....	26
<b>5. ANALYSIS AND CHARACTERIZATION OF ARBITER-BASED PUF</b> ....	<b>29</b>
5.1 Inter-chip Variation .....	29
5.1.1 Information –bearing challenges .....	29
5.2 Environmental Variations .....	32
5.3 Identification/Authentication Abilites .....	33
<b>6. SOFTWARE ATTACKS ON ARBITER-BASED PHYSICAL UNCLONABLE FUNCTION</b> .....	<b>37</b>
6.1 Prediction Tools .....	38
6.1.1 Lineer Programming technique .....	38
6.1.2 Lineer Support Vector Machine .....	40
6.1.3 Radial Base Functions Support Vector Machine.....	41
6.2 Attacks on PUF Circuit Using Linear Programming Aproach .....	43
6.2.1 Experiments with the lineer model of PUF circuit .....	43
6.2.2 Experiments with the PUF on the FPGA .....	44

6.3 Attacks on PUF Circuit Using Support Vector Machine Classifiers.....	46
6.3.1 Experiment with the linear model of the PUF circuit.....	46
6.3.2 Experiments with the PUF on the FPGA.....	47
6.4 The Reason of Differences in Responses between the Linear Model of the PUF and the PUF on the FPGA .....	49
<b>7. CONCLUSION .....</b>	<b>53</b>
<b>APPENDICES .....</b>	<b>59</b>
<b>CURRICULUM VITAE .....</b>	<b>611</b>

## **ABBREVIATIONS**

**POWF** : Physical One Way Function  
**PUF** : Physical Unclonable Function  
**MUX** : Multiplexer  
**SVM** : Support Vector Machine  
**FPGA** : Field Programmable Gate Array  
**LUT** : Lookup Table  
**RBF** : Radial Basis Function



## LIST OF TABLES

	<u>Page</u>
<b>Table 5.1:</b> Table of responses for different PUF circuits against challenges.....	28



## LIST OF FIGURES

	<u>Page</u>
Figure 2.1 : PUF based RFID authentication procedure.....	8
Figure 3.1 : Arbiter-based PUF circuit.....	9
Figure 3.2 : Operation of MUX blocks or switch block components.....	10
Figure 3.3 : Operation of a D-type Flip-Flop and an Arbiter.....	11
Figure 3.4 : Setup and Hold times in a Flip-Flop.....	11
Figure 3.5 : Cell and connect delays in a PUF circuit.....	12
Figure 3.6 : Delays in a switch block.....	13
Figure 3.7 : Configured delay paths with $C_1=0$ and $C_2=0$ control inputs.....	13
Figure 3.8 : Configured delay paths with $C_1=0$ and $C_2=1$ control inputs.....	14
Figure 3.9 : Configured delay paths with $C_1=0$ and $C_2=0$ control inputs.....	14
Figure 3.10 : Configured delay paths with $C_1=1$ and $C_2=1$ control inputs.....	14
Figure 3.11 : Arbiter operation in the example with $m_1$ and $m_2$ path delays.....	15
Figure 3.12 : More general structure of arbiter based PUF.....	15
Figure 3.13 : The symmetrical wiring between two switch blocks.....	16
Figure 3.14 : PUF circuits represented with switch blocks and switch delays.....	17
Figure 4.1 : A Switch block implemented with a MUX.....	22
Figure 4.2 : RTL schematic of a switch implemented with a MUX.....	23
Figure 4.3 : Access the “Property” option of a synthesizer process.....	24
Figure 4.4 : Setting “Keep Hierarchy” parameter to “YES” value.....	24
Figure 4.5 : The D type edge-triggered flip flop.....	25
Figure 4.6 : The VHDL code synthesizing a NAND gate.....	26
Figure 4.7 : The placement of MUX switches in Floorplanner.....	27
Figure 4.7 : Constraints in “UCF” file to select LUT F and LUT G for placement of MUXs.....	27
Figure 5.1 : The density function of the random variable $p_i=\Pr(R_{i,j}(C_i)=1)$ .....	30
Figure 5.2 : The density of the inter-chip variation $y_{i,j}$ for a number of.....	32
Figure 5.3 : The variation of PUF responses due to temperature and power.....	33
Figure 6.1 : Example of solving linear programming problem.....	39
Figure 6.2 : Maximum- margin hyperplane separating classes.....	41
Figure 6.3 : Mapping process for a nonlinear separating surface.....	42
Figure 6.4 : The graph of error rates in prediction of responses by Linear.....	44
Figure 6.5 : The graph of error rates in prediction of responses by Linear.....	45
Figure 6.6 : The graph of error rates in prediction of responses by Linear SVM for the linear model of the PUF.....	46
Figure 6.7 : The graph of error rates in prediction of responses by RBF SVM.....	47

Figure 6.8 : The graph of error rates in prediction of responses by Linear SVM.....	48
Figure 6.9 : The graph of error rates in prediction of responses by RBF SVM.....	48
Figure 6.10 : The last stage of the PUF circuit with the cell and.....	49
Figure 6.11 : Statistical model of delay capturing process variations.....	50
Figure 6.12 : Static delays for last stage of PUF circuit.....	51
Figure 6.13 : Cumulative delay for last stage of PUF with cross connected switch block.....	52
Figure 6.14 : Cumulative delay for last stage of PUF with direct connected switch block.....	52
Figure A. 1: Two successive MUX blocks with delay variables .....	60

## **RELIABILITY AND SECURITY OF ARBITER BASED PHYSICAL UNCLONABLE FUNCTION**

### **SUMMARY**

Modern cryptographic protocols are based on the principle that only authorized people can obtain secret keys and access to information systems. However, various kinds of tampering methods have been devised to extract secret information from smartcards, ATMs and other low-cost electronic devices. In order to resist to cloning and physical attacks physical unclonable functions (PUFs) based on random variations in physical properties of materials were proposed. Using these variations we can obtain unique secret keys. As a result, we no longer need to store the secret keys in digital form. Firstly, this idea was realized using optical micro-structure with bubbles. Then, silicon material was used to realize the Arbiter-based Physical Unclonable Functions (PUFs). This technique exploits statistical delay variation of logic gates across integrated circuits (ICs) due to manufacturing processes to build a secret key unique to each IC. PUF circuits generate a lot of unique, unpredictable, though reliable secret keys from each chip. They are dynamically generated, using a challenge response pairs (CRPs) scheme.

We implemented Arbiter-based PUFs in Xilinx Virtex 2 Pro FPGA and investigated the identification capability, reliability, and security of this scheme. Experimental results show that the internal interconnection in the FPGA leads to asymmetric structure of the PUF circuit which reduces the effect of variations in random component of delays on the responses from PUF circuits. This case lowers the Hamming distance between the responses which directly affects the inter-chip parameter. Environmental noise and inter-chip variation are very important characteristics for the identification process between different PUF circuits. The sources of environmental noise are temperature and voltage variations. The practical range of variations due to the environmental noise shows reliability of the secret keys produced by PUFs on the FPGA. Two different approaches are applied in order to test the resistance of the PUF circuit against software attacks. In the first approach, attacks are considered as a classification problem. Using definite numbers of known CRPs, the classifiers are trying to predict the responses for new challenges. In this thesis, Linear SVM and radial basis function (RBF) SVM classifiers are used. In the second approach, using definite numbers of known CRPs and linear model of PUF circuit, Linear Programming technique is trying to find delay variables.



## **FLIP-FLOP TABANLI FİZİKSEL KOPYALANAMAZ FONKSİYONUN GÜVENLİĞİ VE GÜVENİRLİĞİ**

### **ÖZET**

Modern kriptografik protokoller, sadece yetkili kişilerin gizli anahtar elde edip, sistemdeki bilgiye ulaşabilmesi temeline dayanır. Ancak, akıllı kartlardan, ATM'lerden ve diğer ucuz maliyetli elektronik sistemlerden gizli bilgiyi elde etmek için, çeşitli fiziksel müdahale yöntemleri tasarlanmıştır. Klonlamaya ve fiziksel saldırılara karşı koymak için, malzemelerin fiziksel özelliklerindeki rastgele değişimlere dayanan fiziksel kopyalanamaz fonksiyonlar önerilmiştir. Bu değişimleri kullanarak birbirinden farklı gizli anahtarlar elde edebiliriz. Sonuç olarak, gizli anahtarları sayısal şekilde saklamaya artık ihtiyacımız olmayacaktır. İlk olarak bu fikir içinde kabarcık olan optik mikro yapı kullanarak gerçekleştirilmiştir, sonrasında flip-flop tabanlı PUF gerçekleştirmek için silikon maddesi kullanılmıştır. Bu yöntem her entegre devreye özgü bir gizli anahtar oluşturmak için, entegre devrelerin üretim süreçlerinden kaynaklanan lojik kapıların istatistiksel gecikme değişimleri kullanılmaktadır. PUF devresi her bir yonga için çok sayıda birbirinden farklı, tahmin edilemeyen ve güvenilir gizli anahtar üretir. Bu anahtarlar dinamik ileti cevap çifti yöntemi ile oluşturulmaktadır.

Bu tezde flip-flop tabanlı PUF devresi Xilinx Virtex 2 Pro FPGA'de gerçekleştirilmiştir ve bu yöntemin kimlik belirleme yeteneği, güvenirliliği ve güvenliği incelenmiştir. Deneysel sonuçlar, FPGA içindeki ara bağlantıların, PUF devresini simetrik olmayan yapıya getirdiğini ve gecikme değişiminin rastgele bileşeninin PUF devrelerinden alınan cevaplara etkisini azalttığını göstermektedir. FPGA'ler arası değişimi doğrudan etkileyen bu durum, farklı FPGA üzerindeki PUF devrelerin ürettiği cevaplar arasındaki Hamming mesafesini azaltır. Çevresel gürültü ve FPGA'ler arası değişim, farklı PUF devreleri arasındaki tanımlama süreci için çok önemli özelliklerdir. Çevresel gürültüden kaynaklanan değişimler pratikteki aralığı, FPGA üzerindeki PUF'lar tarafından üretilen gizli anahtarların güvenirliliğini göstermektedir. Bu tezde PUF devresinin yazılımsal saldırılara karşı direncini ölçmek için iki farklı yaklaşım uygulanmıştır. İlk yaklaşımda, saldırılar bir sınıflama problemi olarak ele alınmıştır. Sınıflayıcılar, belirli sayıdaki bilinen ileti cevap çiftlerini (CRPs) kullanarak, yeni girişlere karşı oluşacak cevapları tahmin etmeye çalışmaktadırlar. İkinci yaklaşımda Lineer Programlama tekniği, belirli sayıdaki bilinen ileti cevap çiftlerini ve PUF devresinin lineer modelini kullanarak, gecikme değişkenlerini bulmaya çalışmaktadır.



## 1. INTRODUCTON

Typically, cryptography is used to secure communication between two parties connected by an untrusted network [1]. In such communication, each party has privately stored key information which allows it to encrypt, decrypt, and authenticate the communication. It is implicitly assumed that each party is capable of securing its private information. This assumption is reasonable when a party is a military installation, or even a person, but breaks down completely for low-cost consumer devices. Once a secret key is attained, eavesdropping and impersonation attacks become possible [2].

In low cost devices such as RFIDs and smartcards is essential that sensitive information is safely stored and communicated. However, the inherent power and footprint limitations of such devices, prevent us from employing standard cryptographic techniques for authentication which were originally designed to secure high end systems with abundant power. In practice, the implementation cost of cryptographic hash functions is near that of block ciphers which is around 10K logic gates [3, 4]. For RFIDs the footprint allotted for security is less than 1K gates [5]. Public-key cryptography bears significant computational overhead when compared to secret key techniques. Furthermore, even if the footprint problem is solved, each time an authentication takes place, the device has to transmit large amounts of data through the channel to the reader, which will unnecessarily consume the power of the device.

Another issue of secret key technique is resilience against invasive and non-invasive physical tampering attacks. Laser cutting, microprobing and power analysis have made it possible to extract digitalized secret information from ICs and compromise conditional access systems by using illegal copies of the secret information [2]. Focusing on the problem of invasive attacks, it is apparent that once a device has been opened, the large difference in state between a 0 and a 1 makes it relatively easy to read out the device's digitally stored secrets. Traditionally, such attacks are

avoided by detecting intrusion and erasing the key memory when an intrusion is detected [6]. However, tamper-sensing environments are expensive to produce and, as long as a key is being protected, the intrusion sensors need to be powered, further increasing costs. In order to resist to the cloning and invasive attacks random functions based on the randomness in physical materials were proposed.

Chronology in development of unclonable artifacts shows that the first powerful notion of a physical one-way function (POWF) was introduced by Papu et. al [7]. In the study of the physical one way functions he used transparent optical medium with a 3-dimensional micro-structure containing bubbles. The input-challenge of the POWF is an incoming laser beam and the output (response) is a fixed-length bit vector derived from resulting interference patterns. The interference pattern depends on the angle and frequency of incoming beam and the speckle pattern in the optical medium. After that, Gassend et. al. introduced the concept of a silicon physical unclonable function or silicon PUF [8, 9]. Modern and future silicon technology-based integrated circuits may serve as PUFs due to their intrinsic manufacturing variability. Essentially, a number of unavoidable physical and chemical phenomena, such as silicon lattice imperfection, uneven distribution of dopants, imperfect mask alignment, and non-uniform chemical mechanical polishing, result in gates with sharply different characteristics. Already in 45 nanometer technology, it is common that the delay of the same gate in different ICs differs by 1/3 from the nominal value [7]. Therefore two silicon PUFs, having the same structure and designed to be sensitive to circuit delays, implemented on the same IC or different ICs have different responses to the same inputs.

Since process variation is beyond manufacturers' control, even an adversary who has detailed information of the PUF circuit cannot physically clone the silicon PUF of a given IC. So the authentication in PUF circuits is based on hidden delay or timing information corresponding to a circuit rather than digital information [10]. Since there are several types of PUFs with different structure and complexities from a security point of view (XOR PUF, Feed Forward PUF, and Ring Oscillator PUF) we consider only basic type called arbiter-based PUF.

The main purpose of this thesis is to investigate the reliability and resistance of a PUF, implemented on FPGA, to software attacks. Also, we aim to implement PUF

structures based on MUXs and make analysis on data obtained from them. These data enable us to study the characteristics of the PUFs and sensitivity to changes to environmental factor such as the ambient temperature and voltage variations

This thesis is structured as follows. Chapter 2 defines physical unclonable functions and physical one-way functions, gives an example of one-way mathematical function. Furthermore, in this chapter one of the most common application of PUF is considered.

In Chapter 3 general overview of PUF system and notion of the delays is considered. In this we cover the fundamental components containing in the differential structure of PUF. Also, we show how delay path can be configured using additive property of the delay and underline the conditions that are providing more sensitivity to inherit process variation in PUF circuits. We provide a linear model of PUF circuit where responses are expressed in terms of challenges and delay variables.

Chapter 4 introduces a detailed circuit implementation of arbiter-based PUF on a Xilinx FPGA device using program Xilinx ISE 9.2. We shortly touches on the primitive logic elements that enable us to implement the main components of PUF circuit. Furthermore, the hardware description language codes(VHDL) that generate these components are also given. In this chapter we show how to adjust “synthesize” tool that comes inside Xilinx ISE 9.2 in order to prevent from converting MUX. Also with the integrated in ISE environment “Floorplanner” tool we try to achieve symmetrical placement of switch blocks.

In Chapter 5 the experimental results for PUFs implemented on FPGA are shown. We analyze the important, for security and reliability, characteristics of PUFs such as the inter-chip variation and environmental noise.

Chapter 6 studies the vulnerability of the arbiter-based PUFs against possible software attack models. Based on the linear model we make attacks using a limited number of linear inequalities and linear programming technique. Using this method, we try to solve for unknown delay parameters of the circuit. Then we compare the responses produced by our theoretic model and the model extracted by linear programming algorithm. In the second attack we use artificial neural network. Providing challenge-response pairs for training of the Supported Vector Machine neural networks, the prediction capabilities of these methods are investigated. Also, in this chapter is told about causes of inconsistency between responses of a linear model of a PUF with the responses obtained from FPGA.

Finally, in the last chapter all the parameters that have effects on security of PUF on FPGA are summarized.

## 2. DEFINITION AND APPLICATION OF PHYSICAL UNCLONABLE FUNCTIONS

### 2.1 Definition of One-Way Function

Information security requires a mechanism that provides significant asymmetry in the effort required to make intended and unintended uses of encoded information. Modern cryptographic practice rest on the use of one-way functions(OWF). If  $f$  is one-way function i.e for any argument it is easy to compute but extremely hard to invert, then, even if  $f$  and  $f(PW)$  were made public, it would be nearly impossible for a reasonable adversary to compute the password (PW) from  $f(PW)$ . Here, a reasonable adversary is one that does not have access to exponential computing resources.

Here is the formal definition of one-way functions.

*A function  $f:\{0,1\}^* \rightarrow \{0,1\}^*$  is called strongly one-way if the following two conditions hold[2].*

- Easy to compute: *There exist a deterministic polynomial time algorithm  $A$  such that on input  $x$ ,  $A$  outputs  $f(x)$*
- Hard to invert: *For every probabilistic polynomial time algorithm  $A'$ , every polynomial  $p$ , and all sufficiently large  $n$*

$$\Pr(A'(f(y)) \in f^{-1}(f(y))) < \frac{1}{p(n)} \quad (2.1)$$

Saying that a function  $f$  is easy to compute means that there exist a P-time algorithm  $A$  which, given an input  $x$ , output  $f(x)$ . The second condition means that the probability that algorithm  $A'$  will find an inverse of  $y$  under  $f$  is negligible[1]. Weak one-way functions require only that all efficient algorithms fail with some non-negligible probability.

In order to give an example of OWF candidate let's define a function as  $f(p, q) = p \times q$ , where  $p$  and  $q$  are  $k$ -bit primes and  $*$  is the regular integer multiplication[2]. (So, our domain is the set of pairs of  $k$ -bit primes, and  $f: Pk \times Pk \rightarrow X$  where  $Pk$  is the set of  $k$ -bit primes, and  $X$  is set of  $2 \times k$ -bit numbers). So clearly,  $f$  is not a

permutation. And let's assume that  $n=p*q$ , so that  $f(p, q) = p \times q = n$ . There's no known polynomial time algorithm  $A$  such that  $A(n)$  output values  $p'$  and  $q'$  so that  $p' \times q' = n$ . Of course, we can object this claim offering test all the number from 2 to  $\sqrt{n}$ . And propose a program that works like the following:

*For  $i=2$  to  $\sqrt{n}$  do*

*If ( $i$  divides  $n$ ) then output  $(i, \frac{n}{i})$ ;*

And we would claim that our program runs in time  $O(\sqrt{n})$  which is polynomial in terms of  $n$  [2]. However, keep in mind that the number  $n$  inputted in this algorithm is of magnitude roughly  $2^{2k}$  and of size  $2k$  and since  $\sqrt{n} \approx \sqrt{2^{2k}} \approx 2^k$ , this algorithm runs in time  $O(2^k)$ , which is exponential in terms of input size. Thus this algorithm runs in exponential time. And, no algorithm that's polynomial in terms of  $k$  is known that can factor  $n$ . Therefore, this function  $f$  is easy to compute and difficult to invert.

## 2.2 Definition of a Physical Unclonable Function

Instead of using computational complexity of algorithm, we can exploit the physical randomness in nature, such as heterogeneous optical medium, electrical noise, and process variation in silicon manufacturing, to construct unclonable functions[2]. A physical unclonable function has common properties as one way function but differently it's implemented in a physical device.

Here is a definition of physical unclonable functions based on the definition of one-way functions. The term challenge refers to the input to the functions and response refers to the output [1].

A physical Random Function is the function embodied by a physical device, and maps challenges to responses. A physical unclonable function satisfies the following properties:

- Easy to evaluate: *The physical device can easily evaluate the function in a short period.*

- Hard to predict: *From a polynomial number of physical measurements (in particular, determination of chosen challenge – response pairs(CRPs) ), an adversary who no longer has the device and can only use a polynomial amount of resources (time, matter) can extract only a negligible amount of information about the response to a randomly chosen challenge.*

By the term “easy”, we mean that the function can be computed in polynomial time.

### **2.3 PUF Based RFID Authentication**

PUFs are tiny electrical circuit primitives that exploit the unavoidable IC fabrication process variations to generate unlimited number of unique, unpredictable, though reliable "secrets" from each chip. These secrets are dynamically generated, using a challenge response scheme. A PUF is queried with a challenge vector (input vector) - a random 64-bit (or longer) number. It almost instantly generates a unique response vector (output) - a 64-bit (or longer) number.

In the figure 2.1, an application of PUF based RFID authentication is given [15]. As shown in the figure below, a set of challenge response pairs are collected from the chip, and stored in a database. This may usually happen at an initial stage in the life of the chip, perhaps at a secure location. To authenticate the chip at a later time, one of the stored challenges from the database is sent to the chip, the response generated is compared against the one initially recorded in the database. If the two match, the chip is authentic. Since each chip can have multiple challenge response pairs, each challenge response pair is used just once, as a one-time pad. This prevents replay attacks on PUF authentication.

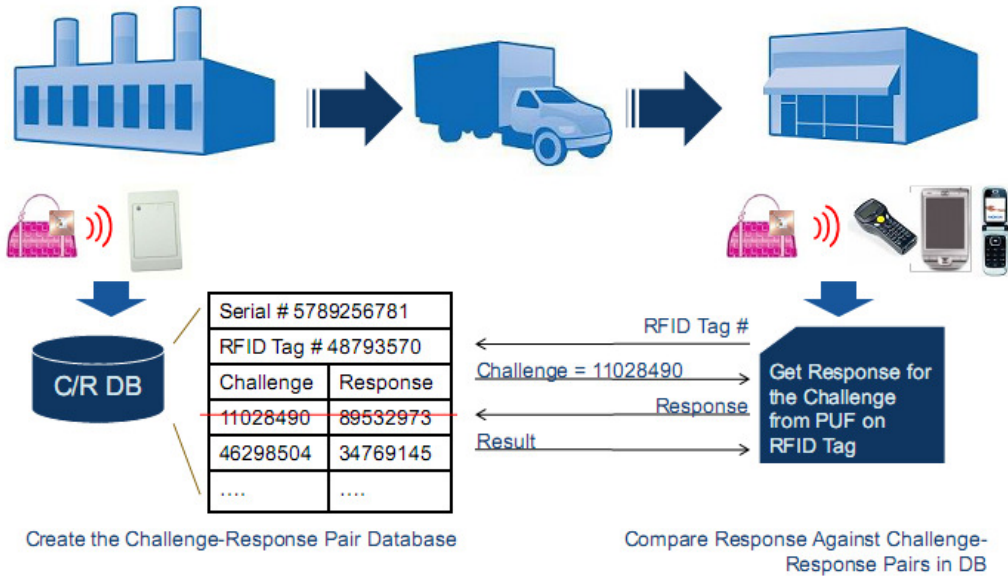


**Figure 2.1 :** PUF based RFID authentication procedure

### 3. DESCRIPTION AND LINEER MODEL OF PUF CIRCUIT

#### 3.1 General Description

An arbiter-based PUF is a  $\{0, 1\}^n \rightarrow \{0, 1\}$  mapping, that takes a n-bit challenge (a) and produces a single bit output (r). The basic idea of a PUF circuit is to create a race between two signals which originate challenge (C) as an input and produces a single bit output (R). The arbiter based PUF circuit consists of n consecutive MUX blocks. Each MUX block consist of two MUXs and has two input and two output bits and a control or select bit. If the control bit of a MUX block is logical 0, the two inputs are directly passed to the outputs through a straight path. However, if the control bit is set to logical 1, the two input signals are switched before being passed to the outputs of the MUX block. Based on the control bit of the MUX block, each of the two input signals will take one of two possible paths. As can be seen from Figure 3.1, there are n MUX blocks where the output of each block is connected to the input of the following block. After the last block, the two output signals are connected to an D Flip-flop. The two inputs of the first block are connected to each other, and the connection is sourced by a pulse generator.

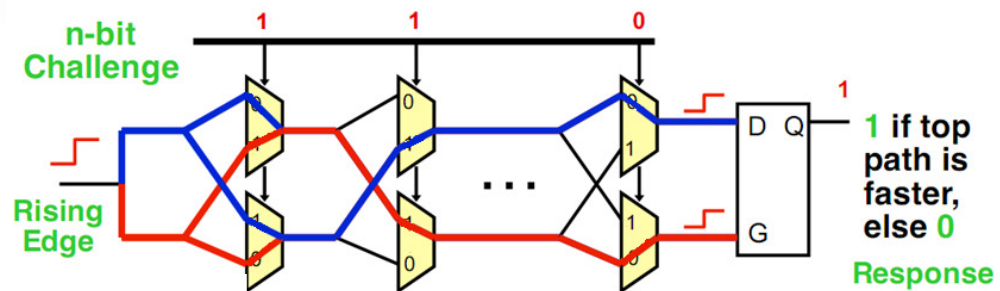


Figure 3.1 : Arbiter-based PUF circuit

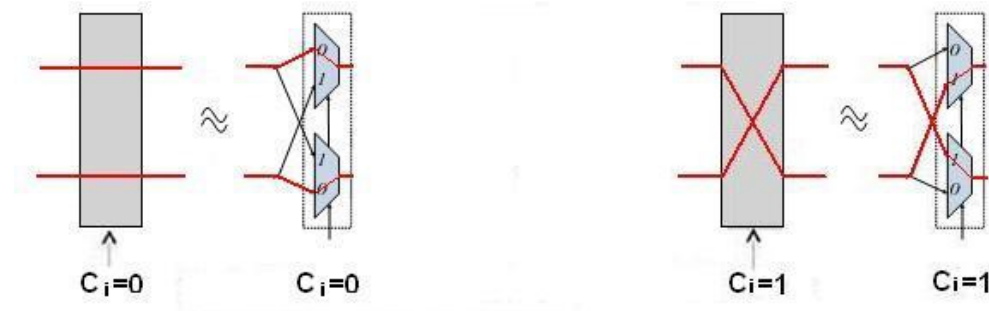
Afterwards, a pulse is generated and fed into the inputs of the first block. Since the inputs of the first block are connected, the pulses traveling through each of the two paths (red and blue lines) are expected to be simultaneous. Although these two paths have been supposed to be perfectly symmetrical, manufacturing variations of these

paths will cause a small mismatch. As the two pulses pass through the consecutive MUXs, they will start acquiring a time delay. The arbiter at the end of the delay paths determines which rising edge arrives first and sets its output to 0 or 1 depending on which of the pulses comming first .

### 3.2 Components of PUF Circuit

As it's seen in the Figure3.1 the main components of PUF circuit are MUX blocks and D-type Flip Flop. Due to their functions they can be represented as a switch block and an arbiter. In the next chapters MUX blocks and switch blocks are used interchangeably. The same is valid for a D-type Flip- flop and an arbiter component.

So, switches as MUX block have 2 inputs, 2 outputs and control or select pins. Applying logic "0" to control pin provide direct connection between input and output which means the signal stay on the same path. On the contrary, if control signal is logic "1" the connection are cross coupled which means the input signals interchange their path. The described operation of switch block component is shown in the Figure 3.2.



**Switch component operation**

**Figure 3.2 :** Operation of MUX blocks or switch block components

A positive edge-triggered D-type flip-flop or arbiter has two input and 1 output pins as it shown in the Figure 3.3. On the positive transition of the clock, the Q outputs will be set to the logic states that were set up at the D input. This logic states are hold until the next transition of clock input.

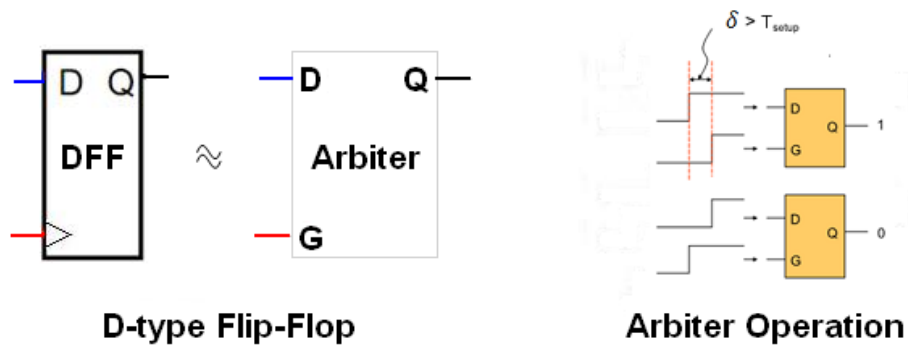


**Figure 3.3 :** Operation of a D-type Flip-Flop and an Arbiter

Flip – flop have setup and hold time that must be satisfied [22]:

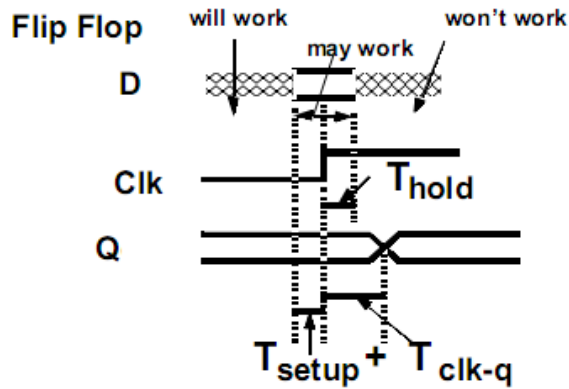


**Figure 3.4 :** Setup and Hold times in a Flip-Flop

If D will arrives before setup time and is stable after the hold time Flip-Flop will work. FF will slow the signal by the setup and “clk to Q” delay in the worst case. In a PUF circuit, if the delay difference between signals in G and D pins is more than setup time,  $T_{\text{setup}}$ , the output will be logic "1", otherwise the output will be logic "0".

### 3.3 Delay Paths in the PUF Circuit

#### 3.3.1 Switch delay

CMOS non-linear model let us define the total (switch) delay of a logic gate i.e the delay between input of the first gate and the input of the next gate as shown in the Figure 3.5[23]. This model propose us to divide the switch delay in two components as cell delay and connect delay which is expressed below by the formula (3.1)

$$D_{switch} = D_{cell} + D_{connect} \quad (3.1)$$

The  $D_{cell}$  delay contributed by the MUX gate itself, is typically defined as the 50 percent input pin voltage to 50 percent output voltage [26]. Cell delay is usually a function of both output loading and input transition time. The connect delay  $D_{connect}$  of an element is the time it takes the voltage at an input pin to charge after the driving output pin has made a transition. In brief, it's the time necessary for a waveform to travel along a wire. The connect delay are the function of wire capacitance, pin capacitance and wire resistance. The wire capacitance and wire resistance are related with wire length.

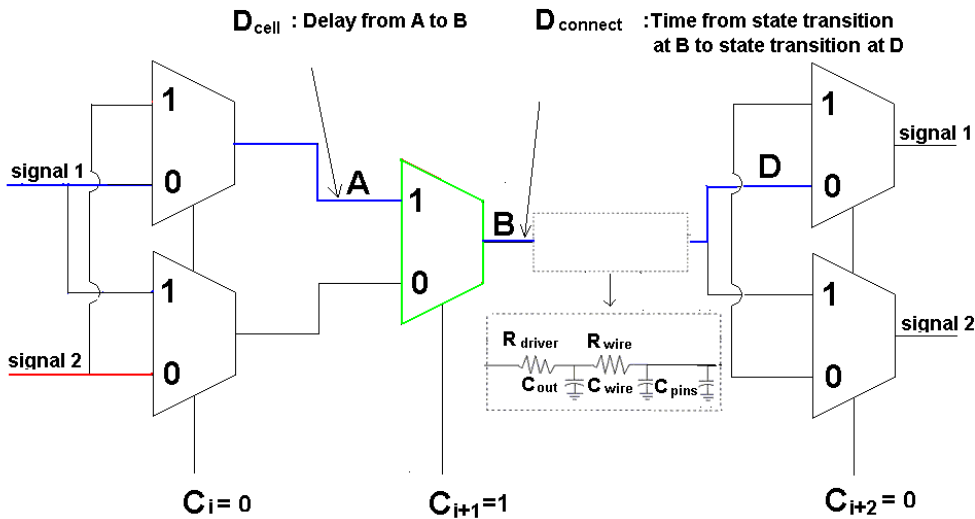
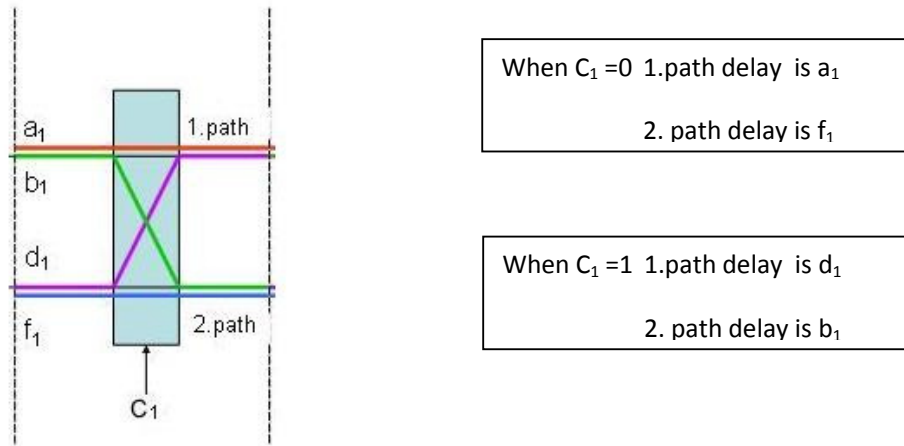


Figure 3.5 : Cell and connect delays in a PUF circuit

### 3.3.2 Delay path configurations

Unique delay paths consist of unique delay of MUXs. Different challenges will impose different paths on the propagating pulses. In order to see different configurations of delay path in PUF circuit we can consider a circuit that consists of two switch components. In this example we assume that the delay behavior's of circuit obeys additive delay model[10].



**Figure 3.6 :** Delays in a switch block

We label the two paths which the upper signal can take as  $a_i$  and  $b_i$ , and for the lower signal as  $d_i$  and  $f_i$ . Paths  $a_1$  and  $f_1$  are chosen when the challenge bit  $c_1$  is 0, whereas  $b_1$  and  $d_1$  are chosen when the challenge bit is 1.

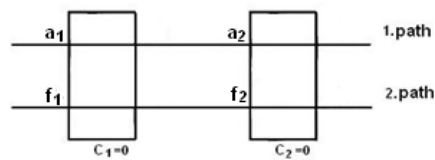


**Figure 3.7 :** Configured delay paths with  $C_1=0$  and  $C_2=0$  control inputs

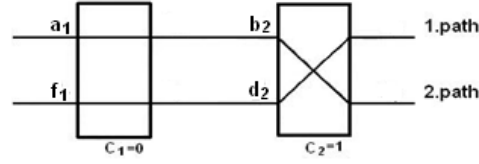


**Figure 3.8 :** Configured delay paths with  $C_1=0$  and  $C_2=1$  control inputs

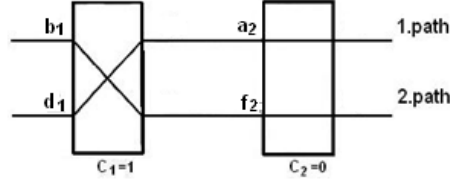


**Figure 3.9 :** Configured delay paths with  $C_1=0$  and  $C_2=0$  control inputs

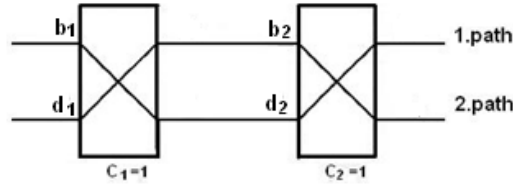


**Figure 3.10 :** Configured delay paths with  $C_1=1$  and  $C_2=1$  control inputs

$a_i, f_i$  is the delays of a signal gained at the end of direct passing through switch to the input of next switch and  $b_i, d_i$  is the delays of a signal gained at the end of cross passing through switch to the input of the next switch .

- For 1. path all set of total delay will be

$$m_{1,1}(b) = a_1 + a_2 \quad (C_1=0, C_2=0) \quad (3.2)$$

$$m_{1,2}(b) = f_1 + d_2 \quad (C_1=0, C_2=1) \quad (3.3)$$

$$m_{1,3}(b) = b_1 + d_2 \quad (C_1=1, C_2=1) \quad (3.4)$$

$$m_{1,4}(b) = b_1 + f_2 \quad (C_1=1, C_2=0) \quad (3.5)$$

- For 2. path all set of total delay will be

$$m_{2,1}(b) = f_1 + f_2 \quad (C_1=0, C_2=0) \quad (3.6)$$

$$m_{2,2}(b) = a_1 + b_2 \quad (C_1=0, C_2=1) \quad (3.7)$$

$$m_{2,3}(b) = d_1 + b_2 \quad (C_1=1, C_2=1) \quad (3.8)$$

$$m_{2,4}(b) = b_1 + f_2 \quad (C_1=1, C_2=0) \quad (3.10)$$

If we set  $C_1 = 0$  and  $C_1 = 1$ , the delay of path 1 is  $m_{1,i} = f_1 + d_2$  and  $m_{2,i} = a_1 + b_2$ . So, if the delay difference,  $\delta$ , between path 2 and path 1 is greater than  $T_{\text{setup}}$  the response will be logic “1”, otherwise the response will be logic “0” as depicted in the Figure 3.10. As we see for  $n=2$  challenges we get  $2 \times 2^2$  different configurations or equations for 1 and 2 path. So if we generalize  $n$  challenge bits lead to  $2^n$  equations for each path with  $4n$  unknown delay variables.

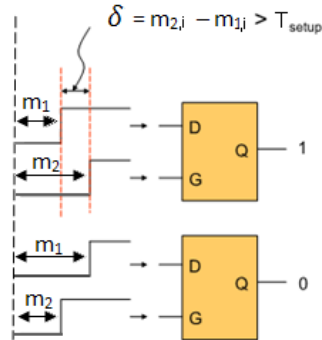


**Figure 3.11** : Arbiter operation in the example with  $m_1$  and  $m_2$  path delays

### 3.4 Symmetrical Structure of PUF circuit

Analyzing the PUF circuit, which is shown in the Figure 3.1, and path delays, which are described in previous section, allow us to propose more general structure of PUF as shown in the Figure 3.11, below:

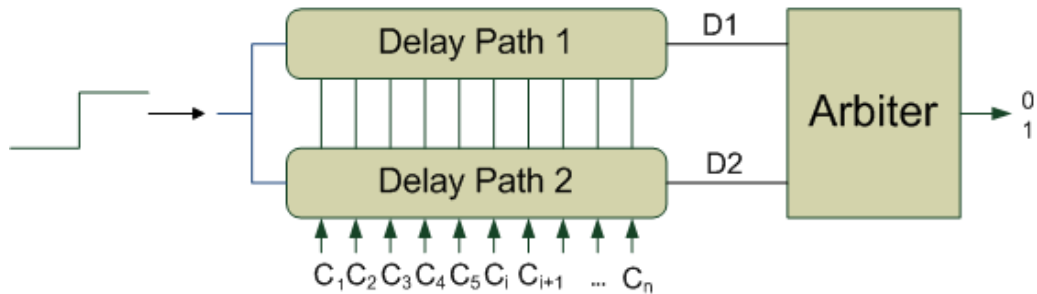


**Figure 3.12** : More general structure of arbiter based PUF

The delay paths are configured by using  $n$ -bit challenge vectors. These challenges select different routing for signals. The signal travelling on this route passing through different switches or MUXes. So, the total delay of signal1 and signal2 at the end of delay paths is sum expression where each entry belongs to unique combination of unique delays. In order to find more general expression for the total delay path 1

and 2 we adds up all the switch delays that signal passing through. After that we separate all switch delays to cell and connect delays components. All this operation are reflected in the formula 3.9 and 3.10. The arbiter gives the output according to measured differences between these delay paths. Formula 3.11 gives the general expression for these difference.

$$D_1 = \sum_{i=1}^{i=n} D_{switch}^{(1)}(C_i) = \sum_{i=1}^{i=n} D_{cell}^{(1)}(C_i) + D_{connect}^{(1)}(C_i) \quad (3.11)$$

$$D_2 = \sum_{i=1}^{i=n} D_{switch}^{(2)}(C_i) = \sum_{i=1}^{i=n} D_{cell}^{(2)}(C_i) + D_{connect}^{(2)}(C_i) \quad (3.12)$$

$$\delta = D_2 - D_1 = \sum_{i=1}^{i=n} (D_{cell}^{(2)}(C_i) - D_{cell}^{(1)}(C_i)) + (D_{connect}^{(2)}(C_i) - D_{connect}^{(1)}(C_i)) \quad (3.13)$$

The last expression show that if difference of connect delay components are much more than difference of cell delay component and setup time of D Flip-flop then the response of PUF circuit are biased to logic "1" or logic "0". As a result the circuit become insensitive to process variations in silicon. That is why we need to reduce the contribution of a connect delay. From section 3.3.1 we know that connect delays are mainly the function of wire length. That's why the only way to do it is to make the structure of PUF symmetric i.e make wire length connecting the MUXs equal. Figure 3.12 help us to depict our statement

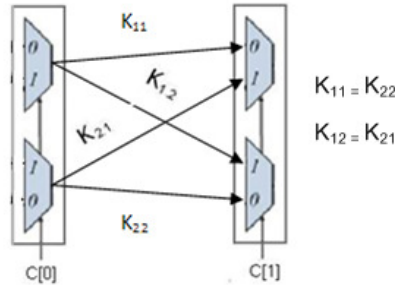


**Figure 3.13 :** The symmetrical wiring between two switch blocks

The symmetrical structure must be maintained through all PUF circuit in order to produce random responses against random challenge vectors.

### 3.5 Linear Model of an Arbiter-based PUF

In this section we derive a linear model for arbiter based PUF [1].

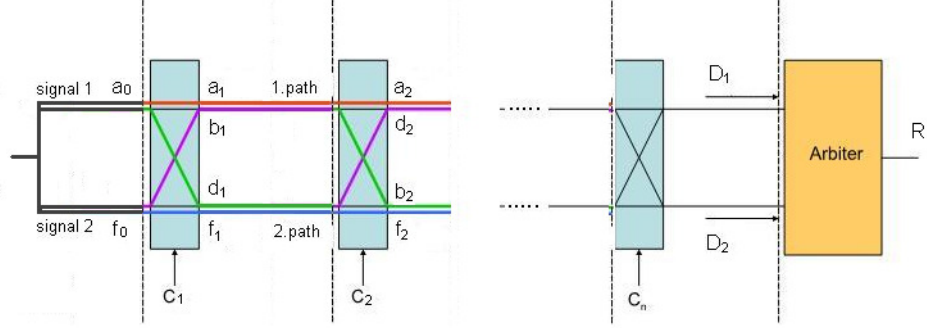


**Figure 3.14 :** PUF circuits represented with switch blocks and switch delays

To compute the total delay, the path of the upper signal is followed from the initial input pulse. The signal will start traveling in a separate path to get to the first switch. Let us label this initial delay as  $a_0$ . For the signal going through the lower path we label this delay as  $f_0$ . In the first switch the delay of the signal 1 will be  $(\bar{c}_1 a_1 + c_1 b_1)$ , where  $\bar{c}_1$  is the complement of  $c_1$ . The delay in the second switch will depend on whether the signals switched paths in the first stage or not. For signal 1 if it doesn't change path ( $c_1 = 0$ ) the delay at switch2 will be  $\bar{c}_1(\bar{c}_2 a_2 + c_2 b_2)$ . If it changes ( $c_1 = 1$ ) the delay at switch will be  $c_1(\bar{c}_2 f_2 + c_2 d_2)$ . So, the total delay of signal 1 at switch 2 will be  $\bar{c}_1(\bar{c}_2 a_2 + c_2 b_2) + c_1(\bar{c}_2 f_2 + c_2 d_2)$ . Let's specify a new variable  $x_i$  which represents the parity of the first  $i-1$  challenge bits, and will signify if the signal starting at the upper path stays in that path or moves to the lower path after  $i-1$  switches. The expression for  $x_i$  is

$$x_i = c_1 \oplus c_2 \oplus \dots \oplus c_{i-1} \quad (3.14)$$

So the delay of  $i$ th switch can be denoted as  $\bar{x}_i(\bar{c}_i a_i + c_i b_i) + x_i(\bar{c}_i f_i + c_i d_i)$

. The total delay in the pulse of signal 1 is

$$D_1 = a_0 + \sum_{i=1}^n \bar{x}_i (\bar{c}_i a_i + c_i b_i) + x_i (\bar{c}_i f_i + c_i d_i) \quad (3.15)$$

Similarly the delay for the signal 2 initiated in lower path can be derived to be equal to

$$D_2 = f_0 + \sum_{i=1}^n \bar{x}_i (\bar{c}_i f_i + c_i d_i) + x_i (\bar{c}_i a_i + c_i b_i) \quad (3.16)$$

The difference between these two delays  $\delta$  is the main variable for our model. This difference will decide whether the output of the PUF is 0 or 1. Since we do not know which of the two signals will end up in the upper path, we will need to incorporate the parity of all the challenge bits which we label P. The difference between the two delays becomes

$$\delta = (-1)^P (D_1 - D_2) = (-1)^P \left( \sum_{i=1}^n (\bar{x}_i - x_i) (\bar{c}_i (a_i - f_i) + c_i (b_i - d_i)) + (a_0 - f_0) \right) \quad (3.17)$$

$$\delta = \left( \sum_{i=1}^n (-1)^{P \oplus x_i} (\bar{c}_i (a_i - f_i) + c_i (b_i - d_i)) + (-1)^P (a_0 - f_0) \right) \quad (3.18)$$

Finally, we define  $v_i = \frac{(a_i + d_i) - (b_i + f_i)}{2}$  and  $u_i = \frac{(a_i - d_i) - (b_i - f_i)}{2}$  for

$i=1 \dots n$  and  $v_0 = (a_0 - f_0)$ . We define the parity of the challenge bits from a reverse order as  $p_i = P \oplus x_i = c_i \oplus c_{i+1} \oplus \dots \oplus c_n$ . The delay equation becomes:

$$\delta = \left( \sum_{i=1}^n (-1)^{p_i} (u_i + (-1)^{c_i} v_i) + (-1)^P v_0 \right) = (-1)^{p_i} u_i + (-1)^{p_i \oplus c_i} v_i + (-1)^P v_0 \quad (3.19)$$

Since connection delays in direct and cross wiring between two following switch boxes ideally suppose to be equal, due to symmetry, we can conclude that the defined variable  $u_i$  must be close to zero. Extracted expressions for  $u_i$  and  $v_i$  variable are given in appendix A. So, in the above expression for  $\delta$  (delay difference) we can omit the parameter  $u_i$ . Note that  $p_1 = P$ , and that  $p_i \oplus c_i = c_{i+1}$ . After defining  $y_i = v_{i-1}$  the final delay equation becomes

$$\delta = \sum_{i=1}^n (-1)^{p_i} (y_i + y_{n+1}) \quad (3.20)$$

Equation (3.20) uses only  $n+1$  rather than  $2n+1$  variables to describe the delay between the upper and lower signal paths. It's important to note that the delay variation  $y_i$  will depend on the fabrication process of the PUF circuit and they denote imbalance in signal propagation paths in  $i^{th}$  stage of the PUF. Therefore, one would expect these variable to follow a normal distribution. Without loss of generality, we can normalize these values and assume they belong to a normal distribution of mean 0 and variance 1. We invoke the arbiter condition for the response bit R. We have

$$\delta > T_s \rightarrow R=1 \quad (3.21)$$

$$\delta < T_s \rightarrow R=0 \quad (3.22)$$

Where  $T_s$  is the setup time for the arbiter.. Finally , we can use Equation to write response equation.

$$(-1)^R \sum_{i=1}^n (-1)^{p_i} (y_i + y_{n+1}) < 0 \quad (3.23)$$

Equation (3.21) is an inequality relating the challenge vector C which consist of n input bits  $C_i$  to the output bit R. This inequality has n+1 variables which characterize the PUF circuit. So, for a single PUF, we may form the following linear equation:

$$\delta_j = (-1)^{p_1^{(j)}} y_1 + \dots + (-1)^{p_2^{(j)}} y_2 + \dots + (-1)^{p_n^{(j)}} y_n + y_{n+1} \quad (3.24)$$

Using Equation 2 we may write the following linear inequality

$$(-1)^{R^{(j)}} [(-1)^{p_1^{(j)}} \quad (-1)^{p_2^{(j)}} \dots (-1)^{p_n^{(j)}} \quad 1] Y < 0 \quad (3.25)$$

where  $Y = [y_1 \ y_2 \ \dots \ y_{n+1}]$



## **4. IMPLEMENTATION OF A PHYSICAL UNCLONABLE FUNCTION ON THE FPGA**

### **4.1 Introduction to an FPGA**

For implementation of PUF circuit we preferred FPGA Virtex2Pro designed and produced by Xilinx Corporation. FPGA devices are preferred to custom IC because of some advantages such as flexibility in reprogrammability and short amount of time for implementation of circuits [11].

FPGAs contain programmable logic components called "configurable logic blocks", and a hierarchy of reconfigurable interconnects that allow the blocks to be "wired together", somewhat like a one-chip programmable breadboard. Logic blocks can be configured to perform complex combinational functions, or merely simple logic gates like AND and XOR. In most FPGAs, the logic blocks also include memory elements, which may be simple flip-flops or more complete blocks of memory [12].

CLB resources include four slices and two 3-state buffers. Each slice is equivalent and contains:

- Two function generators (F&G)
- Two storage elements
- Arithmetic logic gates
- Large multiplexers
- Fast carry look-ahead chain
- Horizontal cascade chain (OR gates)

The function generators F & G are configurable as 4-input look-up tables (LUTs), as 16 bit shift registers, or as 16-bit distributed SelectRAM+ memory. In addition , the two storage elements are either edge-triggered D type flip flops or level-sensitive latches. Each CLB has fast internal interconnect and connects to a switch matrix to access general routing resources [12].

## 4.2 Implementation of PUF components

Xilinx ISE 9.2 is the one of a software tool produced by Xilinx for synthesis and analysis of HDL designs, which enables the developer to synthesize their designs, perform timing analysis, examine RTL diagrams, simulate a design's reaction to different stimulus, and configure the target device with the programmer. In order to synthesize a component and implement it on FPGA we should know the VHDL design flow and understand VHDL codes [13] Any primitive logic are implemented in FPGA by using function generators or look-up tables(LUTs) [12].

### 4.2.1 Switch implemented with MUX

The structure of this switch unit is shown on the Figure 4.1. Each switch unit includes two MUX elements. So this structure enable us to connect directly or cross connect inputs “dI0” and “dI1” to outputs “dQ0” and “dQ1” depending on a challenge input bit .

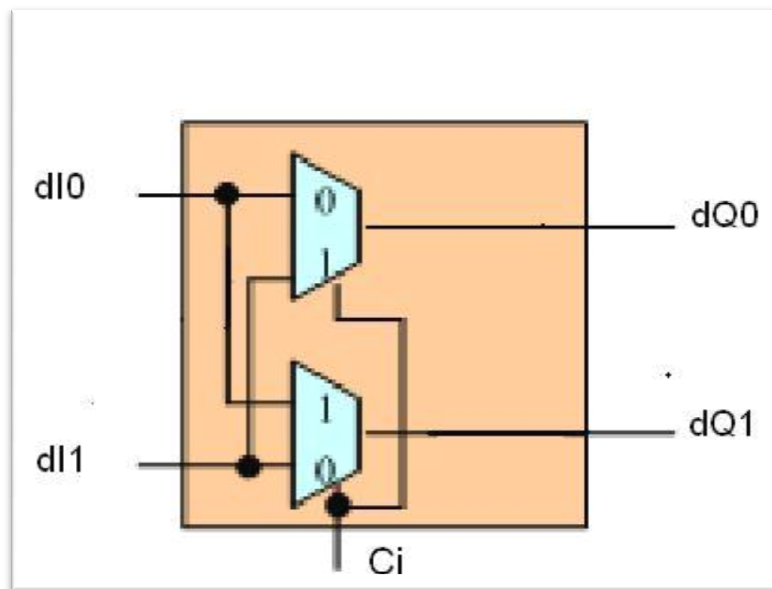


**Figure 4.1 :** A Switch block implemented with a MUX

For synthesis of MUX switch we need to define the entity with three inputs (one of them is challenge bit) and two outputs. Inside of the entity we describe the MUX unit and how they connected. In the architecture part of VHDL codes we define the loop statement “ ”, which is necessary to obtain a chain of

serially connected MUX switch [15] . specifies the number of switches and the size of input vector of challenge bits. The VHDL codes for implementation of switch blocks on FPGA are given in the CD, which is attached with the thesis. As a result of synthesizing this code we get RTL schematic as shown on Figure 4.2.

A Synthesizer integrated in ISE tool always try to optimize the logic. There are usually many ways to implement logic with a given functionality. If the synthesis/mapping/place & route tools recognize that certain blocks do not fulfil a timing requirement, these blocks may be optimized in terms of placement and logic design, possibly at the cost of an increased area or slow speed. That is why as the result of synthesis the MUX gate are simplified and the routing between gates are not as shown in the figure 3.1. To avoid it we must change the constraints of synthesizer as it shown on the figures 4.3, 4.4.

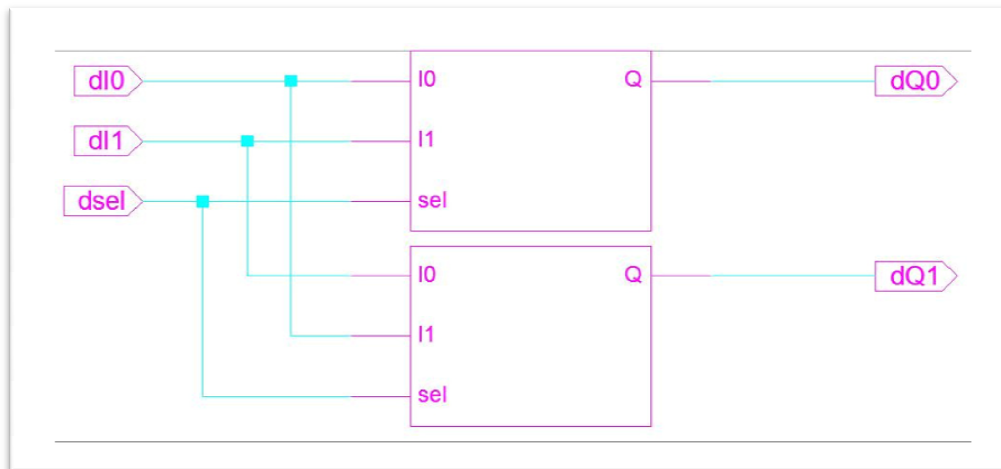


**Figure 4.2 :** RTL schematic of a switch implemented with a MUX

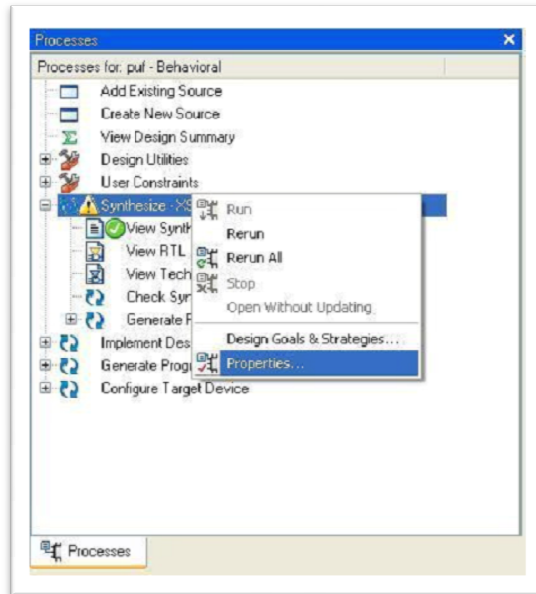


**Figure 4.3 :** Access the “Property” option of a synthesize process

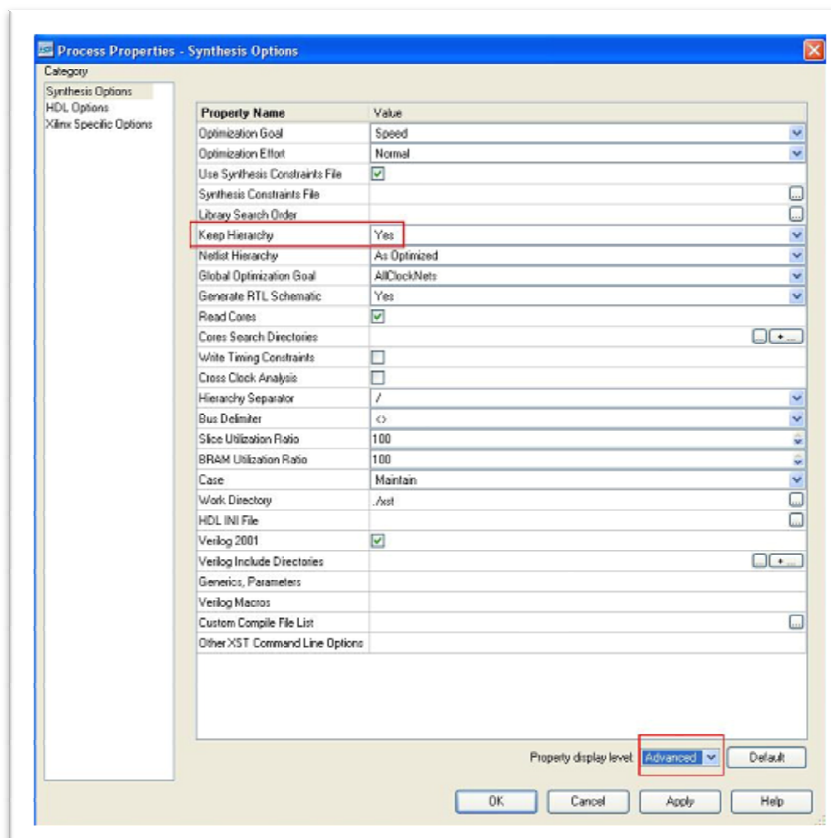


**Figure 4.4 :** Setting “Keep Hierarchy” parameter to “YES” value

### 4.2.2 The Arbiter

For an arbiter we use positive edge triggered D type Flip Flop. Unwilling wiring of clock input of flip flop to an internal system clock signal done by synthesizer make us to implement own D type flip flop. The schematic of the Flip flop are shown on the figure 3.10 [15]

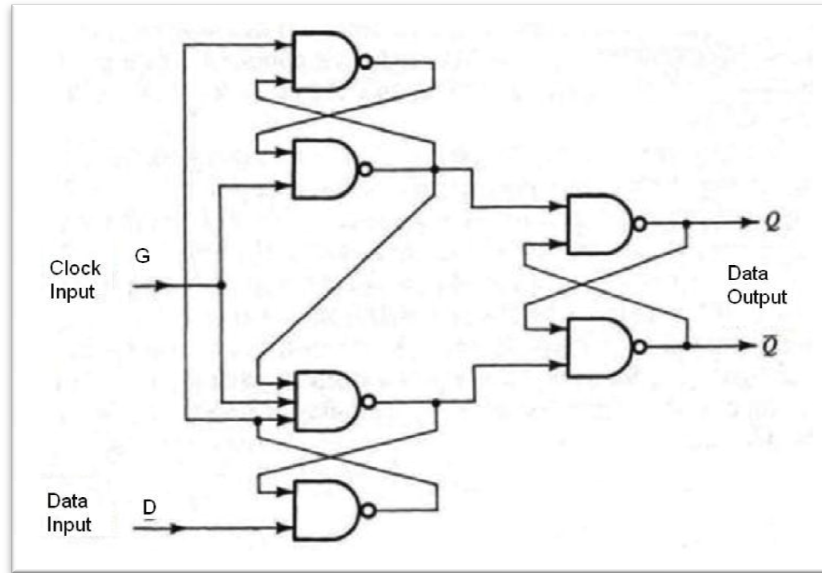


**Figure 4.5 :** The D type edge-triggered flip flop

The operation of D Flip- flop are illustrated in the Figure 3.3. As the rising edge of D comes earlier than that of G, an ideal arbiter output must be 1. However, if the time difference between two signals is less than the setup time of the Flip-flop , an output remains at '0' instead of being switched to '1'. This property introduces an skew factor or imbalance in ratio of numbers of 1 and 0 at the output. The desiring probability of coming '1' or '0' at the output must be the same and equal to 0,5. Frequently most of flip flops favor the path to output '0'. So, to compensate for the skews we fix some of the most significant challenge to effectively lengthen the delay path connected to a gate input [2]. Also, in the graduation project [15] the number of switch blocks or challenge bits, n, giving almost equal rate of logic '1' and logic'0' in response, has been determined experimentally. In this experiment, the responses have been measured against randomly generated challenge vectors. Implementing PUF with n= 64 switch blocks

almost solve our skew problem. In our experiments, with 64 switch blocks we obtain the rate 61 %.

The two signals emitted from the source at the same time after passing through switch blocks arrives to data and clock input of the arbiter. For implementation of the flip-flop shown in figure 4.10 we need a primitive NAND gates. That can be accomplished by configuration of LUT as result of synthesizing the next code:

```
LUT2_inst : LUT2
  generic map (
    INIT => X"7")
  port map ( O => O,
    I0 => I0, -- LUT input
    I1 => I1 -- LUT input
  );
```

**Figure 4.6 :** The VHDL code synthesizing a NAND gate

### 4.3 Placement of Switch Box

In order to maximize the inter-chip variation, the delay path must be placed and routed as symmetrically as possible so as to minimize the delay differences between two paths[1]. Since Xilinx ISE places the gates automatically not considering the wire length or wire delay, the implemented PUF always gives response that biased to logic '1' or logic '0'. So symmetrical placement of switch box minimizing the wire delay shown on the figure 4.12 For that placement we should manually drag and place the MUXs in the according slices that contains this logic gates in Xilinx Floorplanner tool. Having done this placement the tool automatically write this constraint into "ucf" file, which is designated for defining position, time, connection constraints. In this file must be inserted the constraints that fix upper and lower MUXs. In order to keep them close one of them are placed in F LUT the other in G LUT in the according slices. For that we must enter the following codes in "ucf" file shown on the figure 4.13:

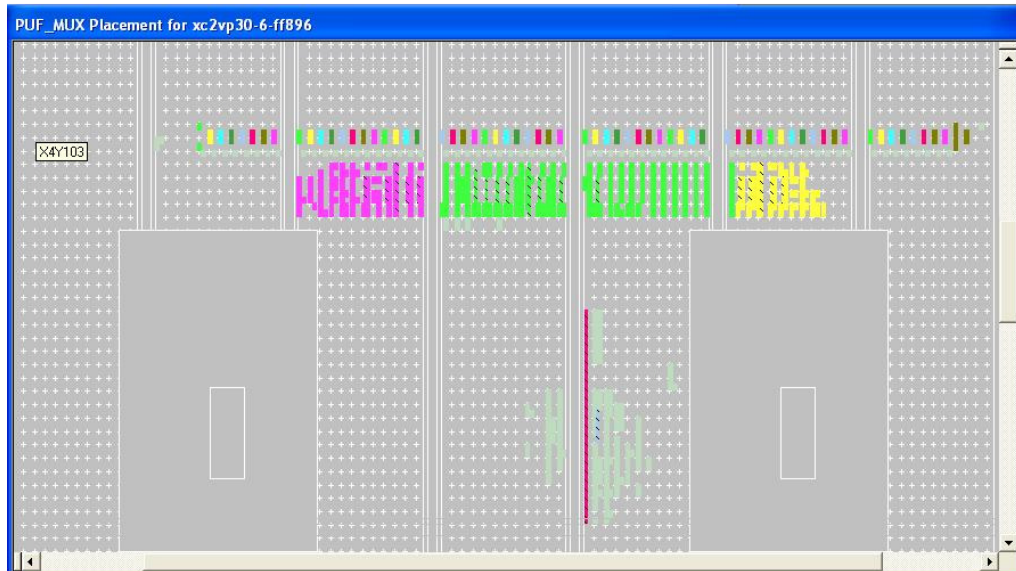


**Figure 4.7 :** The placement of MUX switches in Floorplanner

```
INST "instance_name_upper_MUX" LOC = "SLICE_X20Y5" ;  
INST "instance_name_lower_MUX" LOC = "SLICE_X20Y6" ;  
INST "instance_name_upper_MUX" BEL=G;  
INST "instance_name_lower_MUX" BEL=F;
```

**Figure 4.8 :** Constraints in "UCF" file to select LUT F and LUT G for placement of MUXs



## **5. ANALYSIS AND CHARACTERIZATION OF ARBITER-BASED PUF**

In this section we present the primary characteristics of arbiter-based PUF such as inter-chip variation, measurement noise, and environmental variations, which have important effects on identification process between different PUFs.

### **5.1 Inter-chip Variation**

#### **5.1.1 Information –bearing challenges**

Information –bearing challenges can be defined as the challenges whose responses in a number of different PUFs are not equal. In order to identify a large amount of PUF on FPGA we need considerable numbers of information-bearing challenges. In an experiment where we applied 2000 randomly chosen challenges to 37 chips we could define the ratio of information bearing challenges. Due to the lack of so many FPGAs in our laboratory I decided to make experiments on available two FPGA chips but with different positions of PUF circuit across the FPGA chip wafers. The results of measurements done in another graduation project [2] approve our decision. The results obtained there shows that the variations across different wafers is similar to the variations across one wafer.

Putting the obtained data in matrix form enable us to facilitate some manipulations over data. The entries  $R_{i,j}$  in this matrix are the PUF function  $F^{(j)}$  (corresponding to  $j$  FPGA chip) which takes  $C^{(i)}$  as an input vector.

For each challenges, we have calculated the probability of a response being 1 as follows, in other words we count the occurrence of 1 across a row and divide it by the number of tested FPGA chips or  $j$ .

**Table 5.1 :** Table of responses for different PUF circuits against challenges

Challenges, $C^{(i)}$	Response of each PUF, $F^{(j)}$				
	$F^{(1)}$	$F^{(2)}$	$F^{(3)}$	...	$F^{(h)}$
$C^{(1)}$	$R_{1,1}$	$R_{1,2}$	$R_{1,3}$	$R_{1,\dots}$	$R_{1,h}$
$C^{(2)}$	$R_{2,1}$	$R_{2,2}$	$R_{2,3}$	$R_{2,\dots}$	$R_{2,h}$
...	$R_{i,1}$	$R_{i,2}$	$R_{i,3}$	$R_{i,j}$	$R_{i,h}$
$C^{(v)}$	$R_{v,1}$	$R_{v,2}$	$R_{v,3}$	$R_{v,j}$	$R_{v,h}$

$$p_i = Pr(R_{i,j}(C^{(i)}) = 1) = \frac{k}{19} \quad (5.1)$$

where  $k$  is the number of PUFs that output 1 against each challenge vector  $C^{(i)}$ ,  $i \in \{1,2, \dots, v\}$  and  $j \in \{1,2, \dots, g\}$ . Figure 5.1 shows the density function of the random variable  $p_i$  for 2000 challenges. When  $p_i=0$  or  $p_i=1$ , the challenge does not generate any information since all PUF response are equal. Except for the cases when  $p_i=0$ ,  $p_i=1$ , more than 84 % of the total challenges are information-bearing challenges.

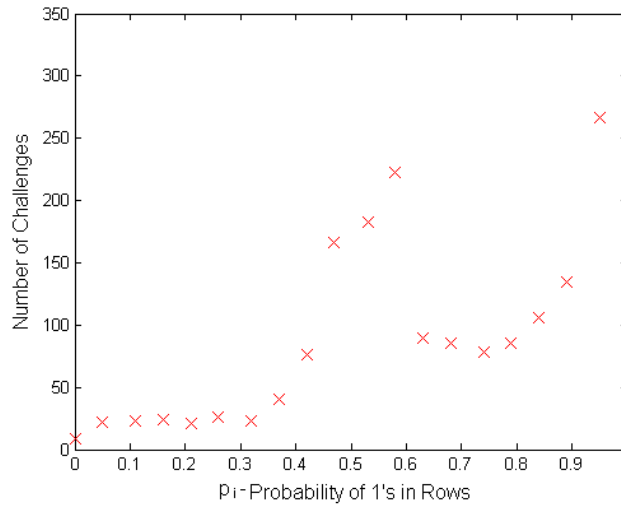


**Figure 5.1 :** The density function of the random variable  $p_i = Pr(R_{i,j}(C_i) = 1)$

The changes in responses of PUFs across a row in the table [2] are resulted from differences in a process variation. The changes in responses of PUFs across a column are arised from different challenges. Definition and evaluation of inter-chip variation

Here we define the inter-chip variation between two different PUFs as below. For two different PUF responses  $R_{i,m}(C_i)$  and  $R_{i,p}(C_i)$  to a challenge  $C_i$  we can define a function that compare the responses which are the inputs to this function. This function behaves like XOR logic function.

$$D_{m,p} = XOR(R_{i,m}(C^{(i)}), R_{i,p}(C^{(i)})) = R_{i,m}(C^{(i)}) \oplus R_{i,p}(C^{(i)}) \quad (5.2)$$

where  $m \in \{1,2 \dots h\}$ ,  $p \in \{1,2 \dots h\}$ ,  $i \in \{1,2 \dots v\}$

Simply by this formula we estimate the Hamming distance between responses of two different FPGAs.

Inter-chip variation is one of the basic functions that make the PUF outputs unique. It is very important for security of PUF based identification. If the PUF produces uniformly distributed independent random bits, the inter-chip variation should be 50% on average [2].

For a random challenge set  $C$ , we define the inter-chip variation  $y_{i,j}$  between PUF  $i$  and  $j$  as

$$y_{m,p} = \frac{1}{|C^{(i)}|} \sum D_{m,p}(C^{(i)}) \quad (5.3)$$

For convenience, we denote the inter-chip variation by  $(100 * y_{i,j})$

Let's assume that our responses from different FPGAs are in matrix or table form as it's shown in the table 1. Finding inter-chip variations between PUF<sup>i</sup> and PUF<sup>j</sup> is equivalent to finding the hamming distance between two columns that corresponds to FPGA with  $i$  index and FPGA with  $j$  index.

We have evaluated  $y_{i,j}$  from 91 arbiter-based PUF pairs using a random challenge set  $C$ , where  $|C|=20000$ . Figure 5.2 shows the density function of 91 evaluated inter-chip variation. Our test-chips have 34% inter-chip variation on average, and the minimum inter-chip variation is 2%. So minimum value of inter-chip is not allowable since it is less than our environmental noise, which will be described in the next section. It means that we can not distinguish any of two different FPGA using these challenges. This PUF based system is vulnerable to impersonation attacks.

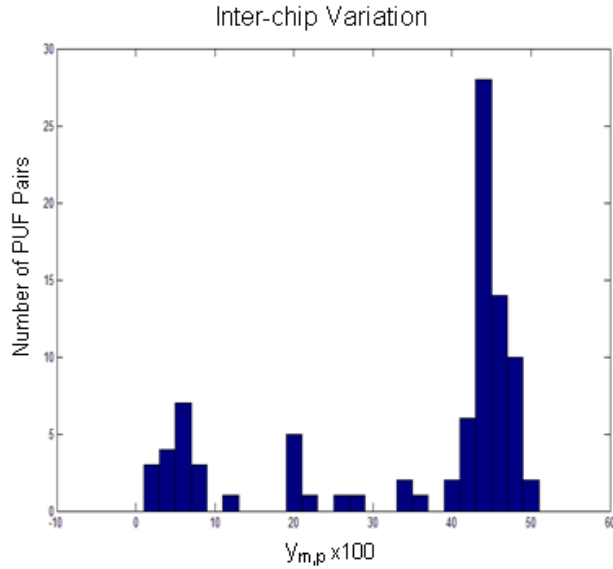


**Figure 5.2 :** The density of the inter-chip variation  $y_{i,j}$  for a number of PUF pairs.

## 5.2 Environmental Variations

Environmental or intra-chip variation is the property that make outputs of a PUF reproducibile. It is important for reliability in applications based on PUFs. We desire 0 % intra-chip variation [15].

Noise, which may cause unreliability in measured PUF responses are arised from temperature and power supply variation [9].

Temperature or power supply voltage variations can significantly change circuits delay and lead to unreliable responses. Since we exploit relative delay measurement, arbiter-based PUFs are robust to such environmental variations. Figure 5.3 shows the amount of environmental variation introduced by temperature ( $\mu_t$ ) and voltage variation ( $\mu_v$ ) . The reference responses are measured at 27 °C and 1,8 V power supply voltage [2]. In this experiments 10000 challenges are used to estimate environmental variations. Even if the temperature increases more than 40 degrees to 70 °C ,  $\mu_t \approx 4,82$  % [2]. Also with  $\pm 2\%$  power supply voltage variation ,  $\mu_v \approx 3,74\%$  .Both  $\mu_t$  and  $\mu_v$  are below the average inter-chip variation.

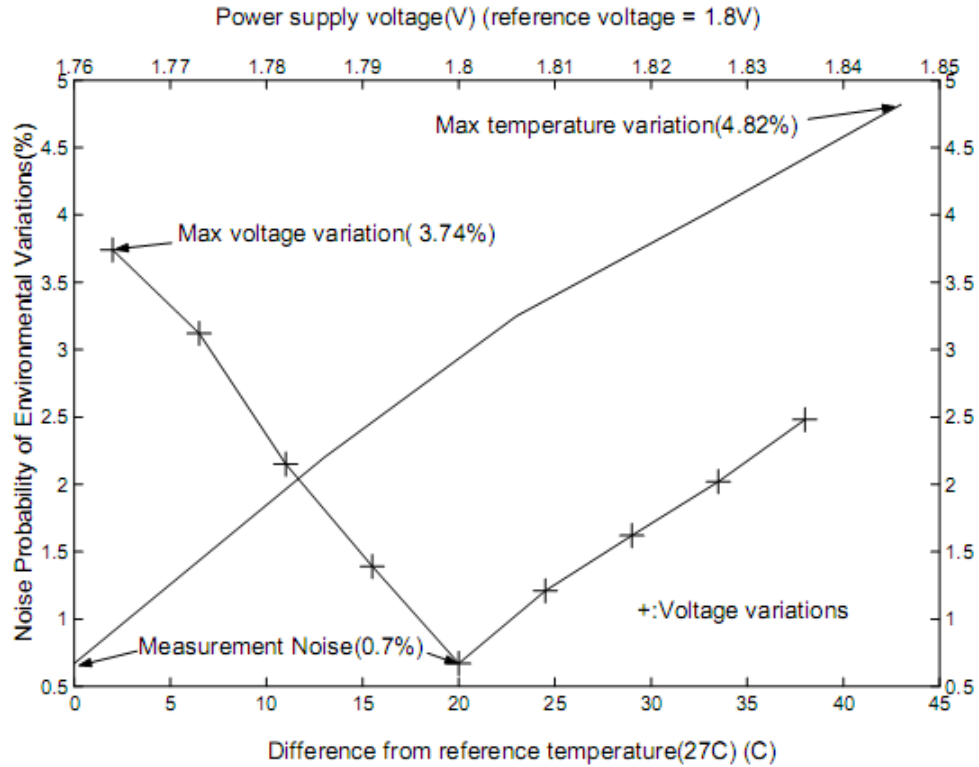


**Figure 5.3 :** The variation of PUF responses due to temperature and power supply changes[2]

### 5.3 Identification/Authentication Abilites

When we use PUFs for the identification of registered users, there exists the server that stores CRP profile of  $N$  registered PUFs in the database. Each CRP profiles has  $k$  CRPs. When a user present a PUF to the server, the server generates CRPs using the presented PUF and compare it with all CRP profiles of the registered users in the database. The server identifies the user by finding the minimum distance CRP profile from generated CRPs of the presented PUF.

In this identification scheme we are trying to find the number  $k$  that enable us to identify  $N=10^9$  different chips with the negligible error probability. It's apparent that before finding the sufficient challenge number  $k$  we need to calculate the number of information bits or delay stages of PUF to distinguish between 1 billion components. The birthday phenomenon will guide us to the right answer. It 's so named because the problem of finding two random challenges which gives the same response value is identical to finding two people in a group of people who share the same birthday

with probability greater than a certain threshold. The probability of one collision is expressed in the next inequality [17]

$$P > 1 - e^{-\frac{n(n-1)}{2m}}$$

where  $n$  - the number of evaluation,  $m$ -possible outputs ( $m=2^l$ ,  $l$  - is the number of information bits)

If we require that the probability of a collision be greater than 0.5, all we have to do is to find that value  $n$  in terms of  $m$  which makes it happen. We found that  $n$  approximately equal to  $m^{1/2}$ . This solution say that in the set of  $m$  possible outputs after  $n$  times evaluation the ouput will repeat with the probability more than 0,5. Therefore  $n$  is the maximum number of times when we can get different output. Similarly in our problem of finding  $l$  information bits to distinguish 1 billion components we need  $m$  (the number of all possible challenges) which is equal to  $n^2$ . So the number of all possible challenges is  $10^{18}$  which is aproximately equal to  $2^{60}$ . Thus to distinguish  $10^9$  chips we need more than 60 information bits.

In the master thesis[1] identification/authentication capability of arbiter-based PUFs based on inter-chip variation  $\zeta$  and noise probability  $\mu$  have been studied. Using  $\zeta=0.22$  and  $\mu=0.048$  the number of sufficient challenges  $k$  is calculated as 443 with error probability  $p_e < \frac{1}{N}=10^{-9}$ . The conclusion that using less than 450 CRPs we can authenticate 1 billions of PUF with negligible probability[2].

To imagine how many combinations can be created with the responses to 450 challenges where the ratio of 1's in 450 bit output vector is 50 % we solve the combination problem where we try to place 225 numbers of 1 in 450 cells. Our expected expression will be

$$Nc = \frac{450!}{225! 225!}$$

The maximum number of components  $Nc$  that can be distinguished by 450 challenges is approximately equal to  $10^{134}$ . In this expression we don't consider inter-chip variations and environmental variations. Including these factors significantly lower this value.

Using the inter- chip factors and measurement noise will make changes to our identification scheme[16]. Suppose that a PUF wants to authenticate itself as Alice. Then the server asks the PUF to generate a list of CRPs corresponding to CRP profile of Alice in server's database. If the PUF is indeed Alice, then each generated response bit differs from the corresponding profile's response bit with probability  $\mu$  . If the PUF is not who it claims to be, then this probability is equal to the inter-chip variation  $\zeta (>\mu)$  .

Inter-chip and intra-chip variation (environmental noise) give us new definitions in identification and authentication process which are false positive and false negative. False positive is probability that PUF A will be authenticated as PUF B when PUF A produce the same output as PUF B. False negative is probability that a correct PUF will fail to be authenticated when PUF fail to regenerate a consistent output [15].



## **6. SOFTWARE ATTACKS ON ARBITER-BASED PHYSICAL UNCLONABLE FUNCTION**

A software attack is one of the non-invasive attacks. It can be realized using the linear programming technique or using machine learning algorithm. In the first case an adversary can formulate the response of a PUF as a function of challenges and delay parameters. If the challenge-response model of the PUF circuit is linear, then an adversary can apply a polynomial number of random challenges and monitor the response to estimate circuit delay parameters in linear model. If the model can predict the response of the circuit with error probability lower than the maximum environmental variation, the adversary can impersonate the original PUF with model. So the main goal of an adversary must be to find out all delay parameters because in this case he could calculate response for any input challenges.

Using Simplex method and Matlab program in linear programming problem we tried to simulate attacks of an adversary. In this attack, Matlab produces random challenges and calculate the responses against each 64 bit challenge. In attack using linear programming approach a certain number of challenge-response pairs or inequalities are used. Simplex algorithm helps us to solve for delay parameters. To analyze the success of this attack we increase the number of input CRPs step by step. The result of attacks using CRPs collected from PUF on FPGA show us the consistency between CRPs created by linear model in Matlab and measured from PUF on FPGA.

The second attack using support vector machine (SVM) classifier, which is one of the machine learning algorithm, show us the possibility to predict the response of challenges in a test set after training the classifier with CRPs in training set. In neural network the feature vectors with 1 and 0 labels are separated by threshold plane.

In the last part of the chapter we mention about causes of failure in linear modeling.

## 6.1 Prediction Tools

In order to make attacks or to find out the all delay parameters of the system having only limited number of CRPs we need calculation tools. Having found all parameters we will able to estimate the response of PUF against each challenge in CRP list of database. This problem can be solved using classification and optimization methods.

We will talk about Simplex algorithm which can be categorized as one of the widely used optimization tools for linear programming model.

The other prediction tool that we will use is based on a machine learning algorithm for classification problem. The classification normally refers to a procedure that learns to classify new instances based on learning from a training set of instances that have been properly labeled by hand with the correct classes. An algorithm that implements classification, especially in a concrete implementation, is known as a classifier. One of the most widely used classifiers is support vector machine (SVMs) classifier [17].

### 6.1.1 Linear Programming technique

A Linear Programming problem is a special case of a Mathematical Programming problem. More formally, linear programming is a technique for the optimization of a linear objective function, subject to linear\_equality and linear inequality constraints. Linear programs are problems that can be expressed in canonical form [18]:

Maximize  $f^T x$

object to  $Ax \leq b$

where  $x$  represents the vector of variables (to be determined),  $f$  and  $b$  are vectors of (known) coefficients and  $A$  is a (known) matrix of coefficients. The expression to be maximized or minimized is called the *objective function* ( $f^T x$  in this case). The equations  $Ax \leq b$  are the constraints which specify a convex polytope over which the objective function is to be optimized. Linear programming can be applied to various fields of study. It is used most extensively in business and economics, but can also be utilized for some engineering problems.

Let's consider a simple example of linear programming (LP) problem [19]:

Find numbers  $x_1$  and  $x_2$  that maximize the sum  $x_1 + x_2$  subject to the constraints  $x_1 \geq 0$ ,  $x_2 \geq 0$  and

$$\begin{cases} x_1 + 2x_2 \leq 4 \\ 4x_1 + 2x_2 \leq 12 \\ -1x_1 + 1x_2 \leq 1 \end{cases} \quad (6.1)$$

In this problem there are two unknowns, and five constraints. The first two constraints  $x_1 \geq 0$ ,  $x_2 \geq 0$ , are special. These are called nonnegativity constraints and are often found in linear programming problems. The other constraints are then called the main constraints. The function to be maximized (or minimized) is called the objective function. Here, the objective function is  $x_1 + x_2$ . We can solve this problem by graphing the set of point in the plain that satisfies all the constraints and then finding which point of this set maximizes the value of the objective function. Each inequality constraint is satisfied by a half-plane of points, and the constraint set is the intersection of all the half-planes. In the present example, the constraint set is the five-sided figure shaded in Figure 6.1

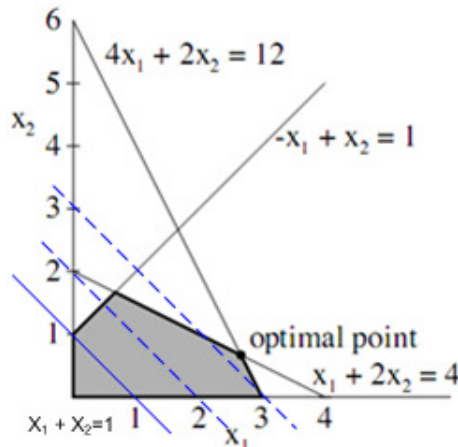


**Figure 6.1 :** Example of solving linear programming problem

We seek the point  $(x_1, x_2)$ , that achieves the maximum of  $x_1 + x_2$  as  $(x_1, x_2)$  ranges over this constrain set. Therefore, we seek the line of slope -1 that is farthest from the origin and still touches the constraint set. This occurs at the intersection of the lines  $4x_1 + 2x_2 = 12$  and  $x_1 + 2x_2 = 4$ , namely  $(x_1, x_2) = (8/3, 2/3)$ . It is easy to see in general that the objective function, being linear, always takes its maximum (or minimum) value at a corner point of the constraint set, provided the constraint set is bounded.

The simplex algorithm, developed by George Dantzig in 1947, solves LP problems by constructing a feasible solution at a corner of the polytope and then walking along a path on the edges of the polytope to corners with non-decreasing values of the objective function until an optimum is reached[19].

For solving LP problems in MATLAB we need Optimization Toolbox including LINPROG routine[20].

### 6.1.2 Linear Support Vector Machine

Given a set of training examples, each marked as belonging to one of two categories, an SVM training algorithm builds a model that predicts whether a new example falls into one category or the other.

Classification is achieved by a linear or nonlinear separating surface in the input space of the dataset. When the feature vectors of the training set are linearly separable by a hyperplane, we can build a linear SVM that uses the structural risk minimization principle to decrease classification errors.

Here we give a description of linear SVM. Let's suppose that we are given training data  $D$ , a set of  $n$  points of the form [21]

$$D = \{(c^{(i)}, s^{(i)}) \mid c^{(i)} \in R^p, s^{(i)} \in \{-1, 1\}\}_{i=1}^n \quad (6.2)$$

where the  $s^{(i)}$  is either 1 or  $-1$ , indicating the class to which the point  $c^{(i)}$  belongs. Each  $c^{(i)}$  is a  $p$ -dimensional real vector. We want to find the maximum-margin hyperplane that divides the points having  $s^{(i)} = 1$  from those having  $s^{(i)} = -1$ . Any hyperplane can be written as the set of points  $c$  satisfying

$$w \cdot c + w_0 = 0 \quad (6.3)$$

where  $\cdot$  denotes the dot product. The vector  $w$  is a normal vector. It's perpendicular to the hyper plane.

We want to choose the  $w$  and  $b$  to maximize the margin, or distance between the parallel hyperplanes that as far apart as possible while still separating data. The hyperplanes can be divided by two equations

$$w' \cdot c + w_0 = 1 \quad (6.4)$$

$$w' \cdot c + w_0 = -1 \quad (6.5)$$

We find the distance between these two hyper planes is  $\frac{2}{\|w\|}$ . So we want to minimize  $\|w\|$ . In some cases, the dataset can not be classified clearly because of non-linearity at the boundary of each class. Considering this case, our goal is not only to make the distance, as large as possible, but also minimize the number of misclassifications.

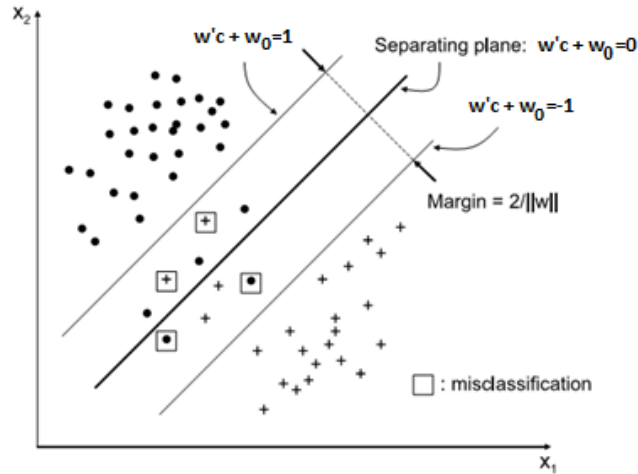


**Figure 6.2 :** Maximum- margin hyperplane separating classes

This is equivalent to minimizing the cost function[2]

$$J(w, w_0, n_e) = \frac{1}{2} \|w\|^2 + \vartheta n_e \quad (6.6)$$

where  $n_e$  is the number of mis-classifications. The parameter  $\vartheta$  is the positive constant reducing of which allows more data to lie on the wrong side of hyper plane and would be treated as outliers which give smoother decision boundary[6].

Lagrangian Support Vector Machines(LSVM) provide fast converging algorithm to the minimal point of the cost function [2].

### 6.1.3 Radial Base Functions Support Vector Machine

There may be another situation where the points are clustered such that the two classes are not linearly separable as shown in the Figure 6.7. In such cases, one prefers non-linear mapping of data into some higher dimensional space called ‘feature space’, where it is linearly separable. The original space of data points is

called ‘input space’. The hyperplane in ‘feature space’ corresponds to a highly non-linear separating surface in the original input space, in the Figure 6.9 [27].

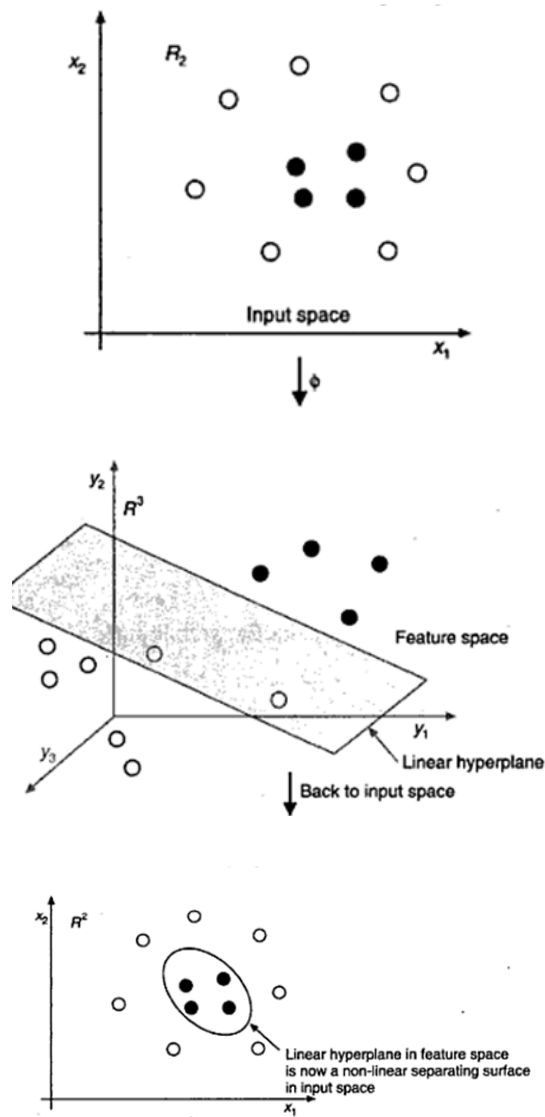


**Figure 6.3 :** Mapping process for a nonlinear separating surface

Given a training  $D$  set of  $n$  data point,  $D = \{(c^{(i)}, s^{(i)}) | c^{(i)} \in R^p, s^{(i)} \in \{-1, 1\}\}_{i=1}^n$  the support vector method approach aims at constructing a classifier of the form [28]:

$$s(c) = \text{sign}[\sum_{i=1}^n \alpha_i s^{(i)} \psi(c, c^{(i)}) + b] \quad (6.7)$$

Where  $\alpha_i$  are positive real constant and  $b$  is a real constant.  $\psi(c, c^{(i)})$  is a row of radial basis function and for RBF SVM can be expressed as  $\psi(c, c^{(i)}) = \exp\{-\|c - c^{(i)}\|^2 / \sigma^2\}$ .  $\psi(., .)$  is also called kernel function and  $\| . \|$  represents a

norm that is generally Euclidean. The known data points  $c^{(i)} \in R^p$   $i=1,2,\dots,n$  are the center of radial basis functions. Radial functions are a special class of function. Their characteristic feature is that their response decreases (or increases) monotonically with distance from a central point. The centre, the distance scale, and the precise shape of the radial function are parameters of the model.

## 6.2 Attacks on PUF Circuit Using Linear Programming Approach

### 6.2.1 Experiments with the linear model of PUF circuit

In this experiment, using definite numbers of known CRPs and the linear model of PUF circuit Linear Programming technique is trying to find the delay variables. After estimation of these delay variables it is easily to obtain new responses for any new challenges. The Linear Programming technique is implemented by the function *linprog* ( $f,A,b$ ), which is included in optimization tool of the Matlab. Let's formulate the linear programming problem one more time:

$$\min f^t x \text{ such that } \begin{cases} Ax \leq b \\ lb \leq x \leq ub \end{cases} \quad (6.8)$$

In our case we need to find  $x$  (delay variables), which must satisfies the constraint inequality  $Ax \leq b$ , where  $b$  is zero vector and  $A$  is matrix with row elements, expressed in the inequality (3.25). Furthermore,  $lb$  and  $ub$  specify the lower and the upper bound for the delay variable correspondingly. We take each element of the vector  $f$  equal to 0, since the objective function is not specified in our case. As a result, optimization problem is turned into constraint solving problem.

Our test are performed for a PUF circuit with  $n$ , number of stages equal to 64. We describe the test procedure step by step below:

- The first step: Matlab produce 50000 random challenge vectors with 64 bit length using unifrom distribution function,  $\text{rand}(1)$ . At the same time, Matlab generate random 65 delay variables. After application of the challenges and random delay variables to the linear model of the PUF we obtain the responses. These responses are saved in a file with according challenges. In this file all CRPs are divided into 2 equal parts which are called train set and test set.

- The second step: We read  $N_s$  CRPs from the train set and transform the challenges to the elements of matrix  $A$  which is used in the  $Ax < b$  expression of the Linear Programming problem.
- The third step: We use these  $N_s$  rows to solve for  $n + 1$  variables. For this purpose the Simplex algorithm are applied.
- The fourth step: We generate 25000 numbers of response using challenges in the test set and the estimated delay variables. Then we compare the responses produced by our model with estimated variables and the responses from the test set. The percentage of errors are given in the Figure 6.4 :

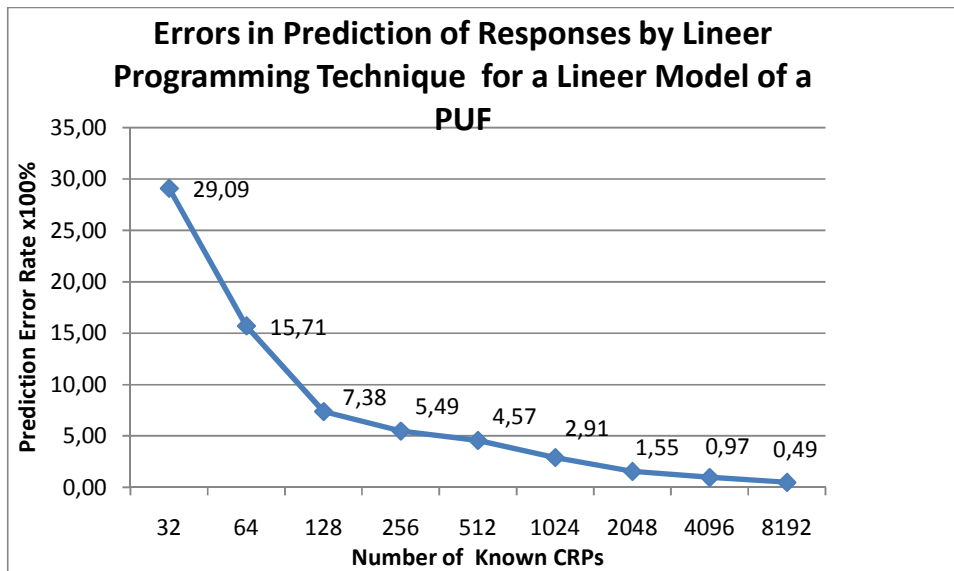


**Figure 6.4 :** The graph of error rates in prediction of responses by Lineer Programming technique for the lineer model of the PUF

In order to identify a chip error rates in prediction of the responses must be less than the environmental noise, which has maximum value 4.82 %. This test shows that to break the PUF scheme we need only 512 CRPs

### 6.2.2 Experiments with the PUF on the FPGA

For the next experiment, CRPs measured from the PUF on the FPGA are used. The applied procedure are given below:

- First step: We produce 50000 random challenge vectors with 64 bits length using uniform distribution function,  $\text{rand}(1)$ . After application of these challenges to the PUF, the measured responses are saved in a file with applied

challenges. In this file all CRPs are divided into 2 equal parts which are called train set and test set.

- Second step: We read  $N_s$  CRPs from the train set and transform the challenges to the elements of matrix A which is used in the  $Ax < b$  expression of the Linear Programming problem.
- Third step: We used these  $N_s$  CRPs to solve for  $n + 1$  variables. For this purpose we use the Simplex algorithm supported by Matlab.
- Fourth step: We generate 25000 numbers of responses using challenges in the test set and estimated delay variables. Then we compare the responses produced by our model with estimated delays and the responses produced by the PUF on the FPGA.

. The percentage of prediction errors are given in the Figure 6.5 .

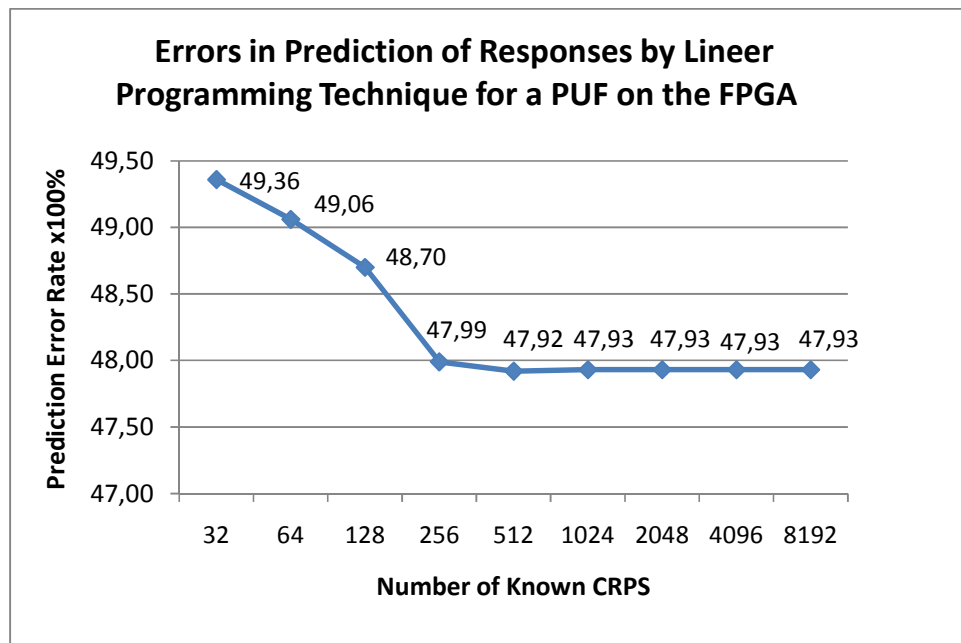


**Figure 6.5 :** The graph of error rates in prediction of responses by Linear Programming technique for a PUF on the FPGA

The results in the Figure 6.5 show that the relation between input vectors and output bits of the implemented PUF doesn't follow the derived linear model, formulated in the inequality 3.23

We will talk about the reason of failure in prediction of responses in the last section of this chapter.

### 6.3 Attacks on PUF Circuit Using Support Vector Machine Classifiers

#### 6.3.1 Experiment with the linear model of the PUF circuit

We performed the test on CRPs generated according to the linear model of the PUF circuit. Our PUF is 64 bits in length . We apply the same test procedure as it has been done in section 6.2.1 . The one difference is that in the third step instead of linear programming technique we are using SVM classifiers. These classifiers are called linear SVM and radial basis function (RBF) SVM because of the linear and RBF kernel functions. As a software tool I have used LIBSVM (Library for Support Vector Machines)tool, which is developed by Chang and Lin[24]. The percentage of prediction error is given in the Figure 6.6 and in the Figure 6.7. These figures show that Linear SVM classifier are more successful than RBF SVM in classification of CRPs generated by the linear model of the PUF.Indeed , in the classification problem, which is implemented by Linear SVM classifier, only definite number of CRPs between 512 and 1024 are enough to break the authentication scheme based on a PUF.However, for RBF SVM classifier we need the number CRPs between 1024 and 2048.

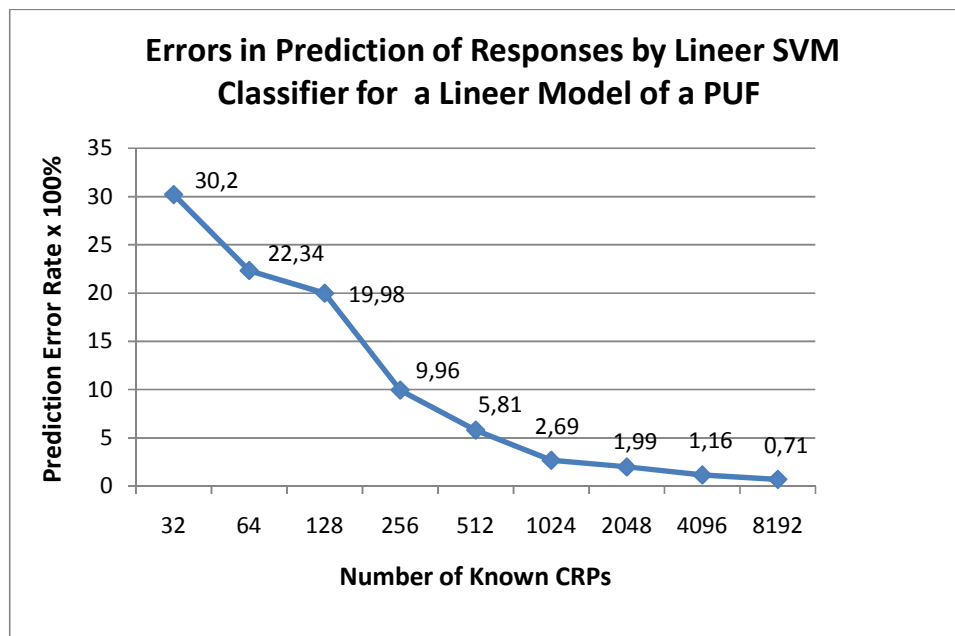


**Figure 6.6 :** The graph of error rates in prediction of responses by Linear SVM for the linear model of the PUF

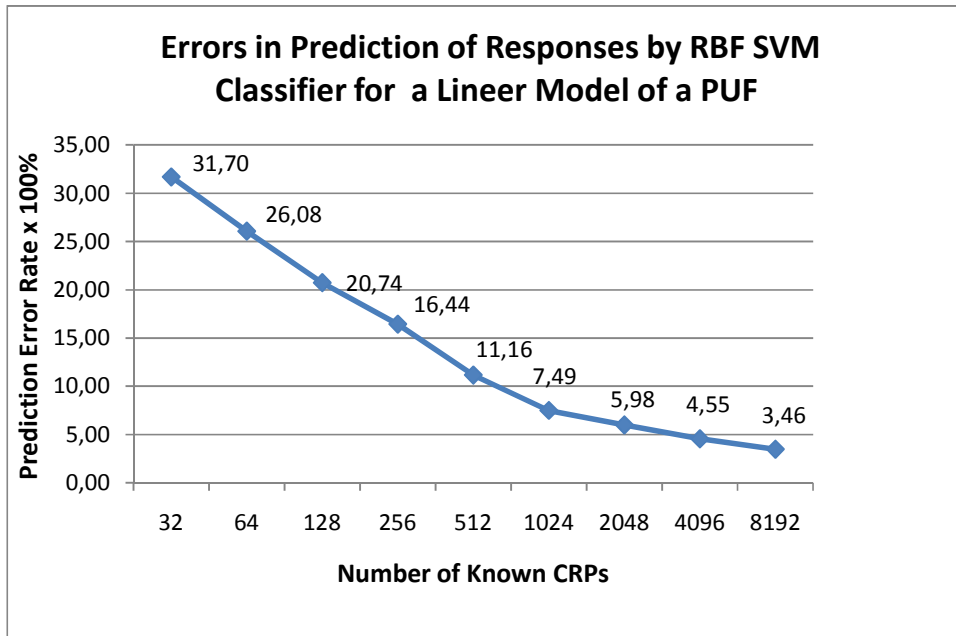


**Figure 6.7 :** The graph of error rates in prediction of responses by RBF SVM for the linear model of the PUF

### 6.3.2 Experiments with the PUF on the FPGA

In order to investigate the success of SVM classifiers in the prediction of responses of the PUF on the FPGA and to compare it with the results for the linear model of the PUF circuit we made an experiment. In this experiment the SVM classifiers are trying to predict the responses for challenges in the test set as it is described in the test procedure given in the section 6.2.2. Instead of linear programming tool we use linear SVM and RBF SVM classifiers. The percentage of prediction errors are given in the Figure 6.8 and in the Figure 6.9. We can see significant differences in prediction errors, given in the Figure 6.6 and in the Figure 6.8. The same is true for the results given in the Figure 6.7 and in the Figure 6.9 or in the Figure 6.4 and in the Figure 6.5. The differences between the results of prediction for the linear model of the PUF circuit and the PUF on the FPGA shows inconsistency between the data.

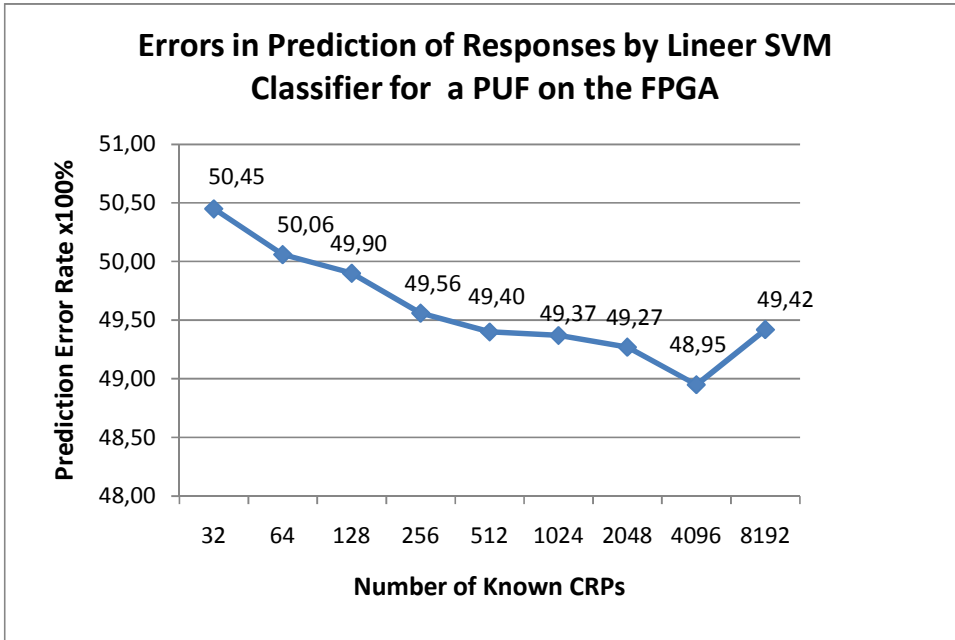


**Figure 6.8 :** The graph of error rates in prediction of responses by Linear SVM classifier for the PUF on the FPGA

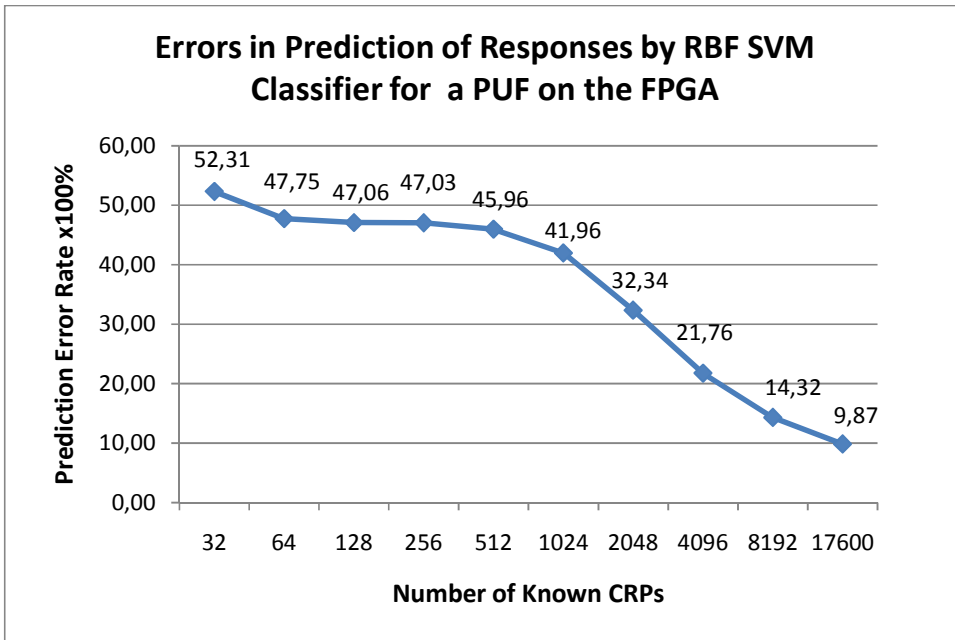


**Figure 6.9 :** The graph of error rates in prediction of responses by RBF SVM classifier for the PUF on the FPGA

In this case RBF SVM classifier are more successful than Linear SVM in the experiments with the PUF on the FPGA. However, in this attack we could not reduce the error rate under environmental noise rate as it is supposed to be in order to succeed. However, this result verify that PUF can be more vulnerable to more sophisticated software that may be already exist or will be developed in near future. Variable resistance to different software attacks is undesirable from the security aspect.

#### 6.4 The Reason of Differences in Responses between the Linear Model of the PUF and the PUF on the FPGA

High error rate in classification problem using SVM classifiers and linear programming approach applied to the data measured from implemented PUF on the FPGA show inconsistency between responses of linear model and responses from the PUF on the FPGA. The result of analysis, made below, approves that we could not satisfy the main condition of symmetry in implementation of the PUF circuit on the FPGA.

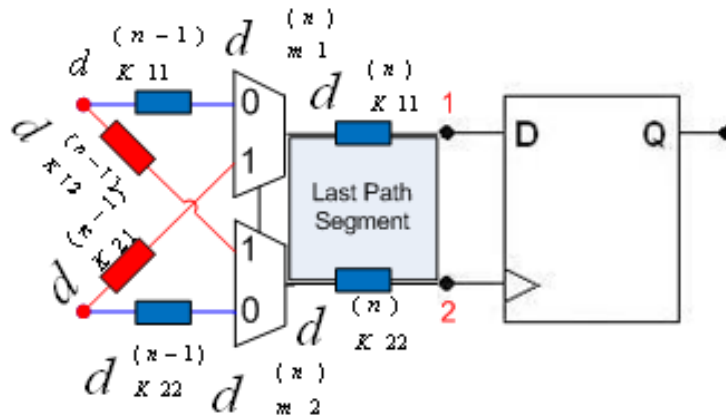


**Figure 6.10 :** The last stage of the PUF circuit with the cell and the connect delays

To identify the critical path in a design and to check whether the timing constraints could be fulfilled, timing analysis tools are used. This tool uses the difference between required time and actual path delays. Actual path delays which consist of the delay of the design elements and interconnects are read from SDF ( Standard Delay Format) file. If we use approach of statistical static timing analysis all the delays can be described in terms of mean and standart deviations as it is shown on

the Figure 6.9[25] . Worst case operating condition corresponds to the extreme  $3\sigma$  corners in the Figure 6.11. So, in the statistical timing model any delay can be separated as a static delay component and a random delay component. Random delay component are caused by process variation which can reach 3,5 % of nominal (mean) value [26] and refer to  $3\sigma$  corner in statistical delay model.

For investigation of effect of static delay and random delays on the response of PUF we can use the figure (6.8). Proceeding from previous knowledge let us write expressions for delays at point 1 and point 2 as it is done in the expression (6.7) and (6.8). The result of PUF circuit will depend on the difference  $\Delta d$  ,which is expressed in (6.9)

$$d_1 = d_{1,s} + d_{1,R} \quad (6.9)$$

$$d_2 = d_{2,s} + d_{2,R} \quad (6.10)$$

$$|\Delta d| = |d_1 - d_2| = |\Delta d_s + \Delta d_R| \quad (6.11)$$

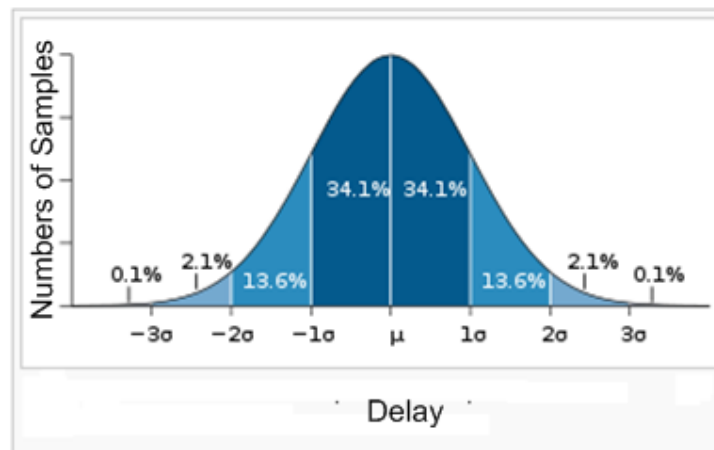


**Figure 6.11 :** Statistical model of delay capturing process variations between ICs

From the Figure 6.10 we can derive expressions for  $d_{1,s}, d_{2,s}, d_{1,R}, d_{2,R}$  is a function of  $d_{K11}^{(n-1)}, d_{K21}^{(n-1)}, d_{K11}^{(n1)}$  and  $d_{m1,S}^{(n)}$

$$d_{1,s} = \overline{C_n} d_{K11}^{(n-1)} + C_n d_{K21}^{(n-1)} + d_{K11}^{(n1)} + d_{m1,S}^{(n)} \quad (6.12)$$

$$d_{2,s} = \overline{C_n} d_{K22}^{(n-1)} + C_n d_{K12}^{(n-1)} + d_{K11}^{(n1)} + d_{m2,S}^{(n)} \quad (6.13)$$

$$d_{1,R} = d_{m1,R}^{(n)} \quad (6.14)$$

$$d_{2,R} = d_{m2,R}^{(n)} \quad (6.15)$$

In the figure (6.12) the result of asymmetry in wiring cause a big differences between static delays of path 1 and path 2 before the arbiter.. By using these equations and static or mean delay form timing analysis we can find cumulative delay at point 1 and 2 . The result are graphycally displayed in the figure (6.13) and (6.14). From the figure (6.13) we find the ratio of static component to random component as  $\Delta d_S / \Delta d_R \approx 50$  and from the figure(6.14)  $\Delta d_S / \Delta d_R \approx 0.4$ . As it is seen from the figure (6.14), in direct connection of switch block the response of PUF are not determined by  $\Delta d_R$  but  $\Delta d_S$  since  $\Delta d_S$  value are considerably more than  $\Delta d_R$ . In the figure (6.13), the value of  $\Delta d_S$  is less than  $\Delta d_R$  which means that our response are completely depends on random process variation.

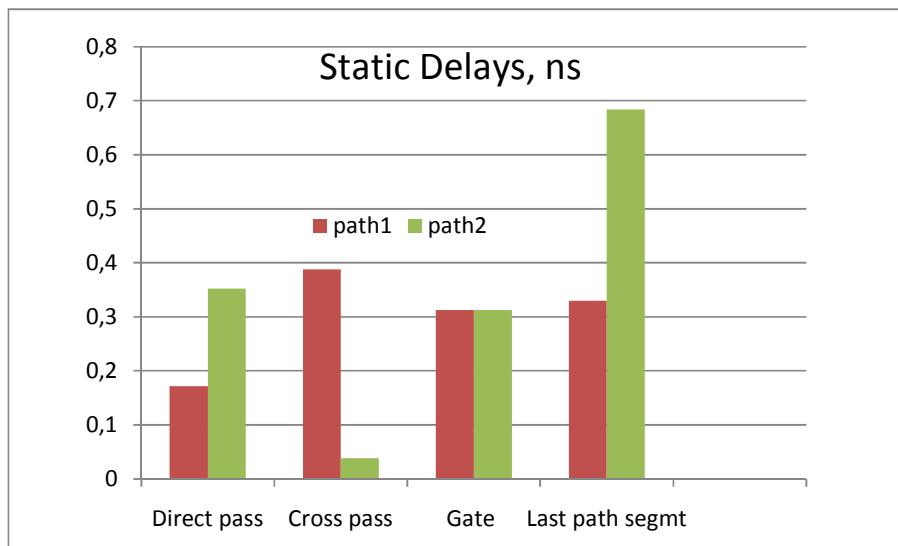


**Figure 6.12 :** Static delays for last stage of PUF circuit

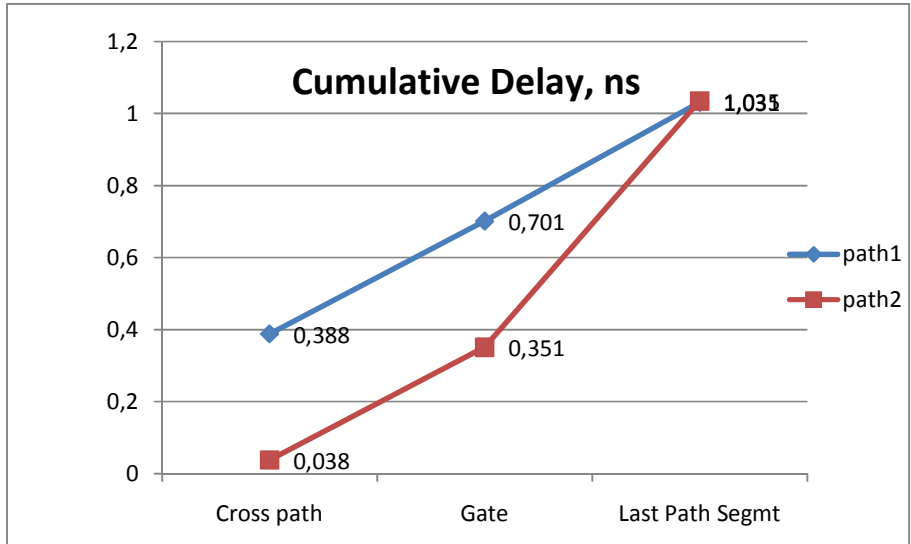


**Figure 6.13 :** Cumulative delay for last stage of PUF with cross connected switch block

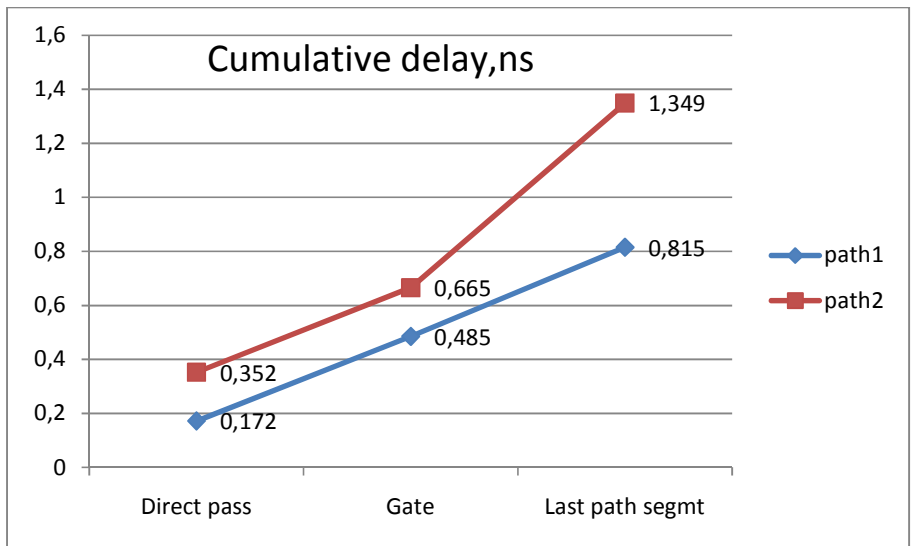


**Figure 6.14 :** Cumulative delay for last stage of PUF with direct connected switch block

## 7. CONCLUSION

In this thesis we have investigated the security and reliability for arbiter-based PUF circuit and conducted preliminary experiments. By using authentication method based on PUF circuit it is possible to store secrets on a chip that is less vulnerable to invasive attacks than traditional digital methods.

We have implemented arbiter-based PUF using MUX on Xilinx Virtex 2 Pro FPGA. Experiment results have shown that there are enough variation between programmable gates not only on different FPGA chip but also on the same chip for identification purposes. The undesired effect of temperature and power supply voltage variations can change the delay characteristic of PUF circuit making worse the reliability parameter. Experiments of applying different challenges to PUFs circuit which are in different position across FPGA chip show that not any challenge can be used for identification purposes. Some of the challenges produce the same outputs in different FPGA circuits. The asymmetry in wiring reduce the numbers of challenges that provide high inter-chip variations.

We have tested the security of linear model PUF circuit, described by equation in section 3.5, against software attacks. For this purpose we have used the linear model the security analysis of linear model created in Matlab suggest that the device could be vulnerable to model building software attack. In fact, we see that

Our experiments where we use the responses produced by linear model and response measured from implemented PUF have shown different resistance to software attacks. In linear model, 1024 CRPs is enough to solve for all delay variable or to predict the outputs for any next challenges. However, linear programming and linear SVM haven't succeeded in prediction of responses, which bring the fact of inconsistency between responses of the linear model and the responses measured from FPGA. Delay analysis report presented by Xilinx Timing Analyzer tool have shown that in spite of symmetrical position arrangement of MUXs across a chip we could not achieve desired symmetry in wire delays between switch blocks. It lead to corruption of responses in the PUF on the FPGA. In spite of that, application of

SVM using radial based kernel have considerably increased prediction rate up to 90 percent where we need 17600 CRPs for a training procedure. This fact verify that PUF based system can be vulnerable to more sophisticated attacks, which is unacceptable from the security aspect. Especially in case of man in the middle attack. Since authentication process of PUF occurs in untrusted and open environment the adversary can easily collect the data, which will be used for software attacks. More authentication process provides him more CRPs. The low intra-chip variation can complicate the aim of adversary since in this case we need more CRPs to train our machine learning algorithm.

In order to prevent the predictions of responses, we can employ non-linear arbiters such as feed-forward arbiter PUFs. It is difficult for an adversary to build an appropriate software model of these arbiters [1].

## REFERENCES

- [1] **Erdinç, Ö., Ghaith, H. and Berk, S.**, 2008: Toward robust low cost authentication for pervasive device. In: *PERCOM '08 Proceedings of the 2008 Sixth Annual IEEE International Conference on Pervasive Computing and Communications*; Hong Kong, China ;17-21 March, pp.170-178.
- [2] **Daihyun, L.**, 2005: Extracting secret key from integrated circuits ,*M.Sc. Thesis*, Massachusetts Institute of Technology, Cambridge, MA, May 20.
- [3] **Feldhofer, M., Dominikus, S., and Wolkerstorfer, J.**,2004: Strong Authentication for RFID Systems Using the AES Algorithm. In: Proceeding of the *Six International Workshop on Cryptographic Hardware and Embedded Systems (CHES 2004)*, Cambridge, MA, USA, August 11-13, 3156 vol. of LNCS, pp. 357–370.
- [4] **Kaps , J.-P., Sunar, B.**, 2006: Energy Comparison of AES and SHA-1 for Ubiquitous Computing.In:Proceedings of the *EUC-06 Workshop on Embedded and Ubiquitous Computing* , Seoul, Korea, 1-4 August, vol. 4097 of LNCS, pp. 371-382.
- [5] **Poschmann,A., Leander, G., Schramm, K., Paar ,C.**, 2006: A Family of Light-Weight Block Ciphers Based on DES Suited for RFID Applications.In: *Proceeding of FSE 2006 on RFID Security*, Graz, Austria. 12.-14. July
- [6] **IBM**, 2009: IBM 4764 PCI-X Cryptographic Coprocessor Custom Software *Interface Reference Release 3.30*, June 11. Available from: <http://www-03.ibm.com/security/cryptocards>.
- [7] **Beckman, N., and Potkonjak M.**,2009:Hardware-Based Public-key Cryptography with Public Physically Unclonable Functions .Revised Selected Papers :*11th International Workshop on IH 2009*, Darmstadt,Germany, June 8-10, vol. 5806 of LNCS, p.206-220
- [8] **Gassend B.**,2003: Physical Random Functions, *M.Sc. Thesis*, Massachusetts Institute of Technology, Cambridge, MA, Jan. 2003.
- [9] **Gassend, B., Clarke, D., Van Dijk M., and Devadas S.**, 2002: Silicon Physical Random Functions . In : Proceedings of the *9th ACM Conference on*

*Computer and Communications Security (CCS'02)*, Washington, DC, USA, November 18 - 22,

- [10] **B.Gassend, D.Clarke, M.van Dijk and S.Devadas.** 2003 Delay-based Circuit Authentication and Application. In: *Proceedings of the 2003 ACM Symposium on Applied Computing (SAC'03)*, Melbourne, Florida, USA, March 09 - 12, p.294-301
  
- [11] **Patra, A., Mall, R., Routray, A,** 2011. *WebCourse 20* : Field Programmable Gate arrays and Applications, Embedded Systems.  
Available from : [www.scribd.com/doc/31436874/FPGA](http://www.scribd.com/doc/31436874/FPGA)
  
- [12] **Xilinx,** 2007: Virtex-2 Pro and Virtex-2 X Platform FPGAs, *Complete Data sheet*, November 5
  
- [13] **Pedroni, A. V.,** 2004 :Circuit Design with VHDL, MIT Press Cambridge, Massachusetts, London, England
  
- [14] **Ozturk, E., Hammouri, G., Sunar, B.,** 2008: Physical unclonable function with tristate buffers. In: *Proceedings of the International Symposium on Circuits and Systems (ISCAS 2008)*, Seattle, Washington, USA, 18-21 May, pp. 3194-3197
  
- [15] **Soybali, M.,** 2010: Implementation of Reliable RFID Applications , *Undergraduate Thesis*, Istanbul Technical University, Istanbul, Turkey, May 2010
  
- [16] **Pappu, R., Recht, B., Taylor, J., Gershenfeld, N.,** 2002: Physical One-Way Functions, *International weekly science journal* ,vol. 297 no. 5589, pp. 2026-2030 , 20 September
  
- [17] **Duda, O. R., Hart, E.P., Stork, G.D.,** 2000: *Pattern Classification*, Second Ed., John Wiley & Sons Inc, November
  
- [18] **Chvatal, V.,** 1983: *Linear Programming* , W.H.Freeman & Company
  
- [19] **Katta G. Murty,** 1983: *Linear Programming*, John Wiley & Sons
  
- [20] **Dantzig, G.B., A. Orden, and P. Wolfe,** 1955: Generalized Simplex Method for Minimizing a Linear Form Under Linear Inequality Restraints, *Pacific Journal Math.*, Vol. 5, pp. 183–195
  
- [21] **J.P.Lewis,** 2004: Tutorial on SVM, CGIT Lab, U.Southern California, USA

- [22] **Saleh, R.**, 2009: Flip-Flop and Clock Design, *Lecture 6 of course "Advanced Topics in VLSI Design*, The university of British Columbia,  
Available from: [www.ece.ubc.ca/~elec579/clockflop.pdf](http://www.ece.ubc.ca/~elec579/clockflop.pdf)
- [23] **Jeyaraman, V.**, 2004: Design ,Characterization and Automation of Ultra-high Temperature Standard Cell Library for Harsh Environment , *M.Sc. Thesis*, University of Madras, Chennai, India, December 2004
- [24] **Chih-Chung Chang and Chih-Jen Lin**,2011: LIBSVM : A Library for Support Vector Machines, *Implementation document* , National Taiwan University, Taipei, Taiwan, February 10
- [25] **Chadha , R.,, Bhasker ,J.**,2009: Statistical Static Timing Analysis-A Better Alternative, *EE Times Design electronic newsletters*,2/3/2009  
Available from: <http://www.eetimes.com/design/eda-design/4018791/Statistical-Static-Timing-Analysis--A-Better-Alternative>
- [26] **Morozov, S., Maiti, A., and Schaumont, P.**, 2010: An Analysis of Delay Based PUF Implementations on FPGA. In:Proceedings of *the 6th International Symposium on Reconfigurable Computing: Architectures, Tools and Applications*, Bangkok, Thailand, March 17-19, 2010, 5992 vol. of LNCS, pp. 382–387
- [27] **Soman, K.P., Ajay ,Y., Loganathan, R.**, 2009: Machine Learning with SVM and Other Kernels, PHI Learning Pvt. Ltd, New Delhi , India ,p.122-124
- [28] **SUYKENS ,J.A.K. and VANDEWALLE, J.**,1999: Least Squares Support Vector Machine Classifiers, *Neural Processing Letters* , Vol. 9 Issue 3: 293–300, June 1999



## **APPENDICES**

### **APPENDIX A.1: Extraction of Expressions for $u_i$ and $v_i$ Variables in the Equation 3.17**

## APPENDIX A.1

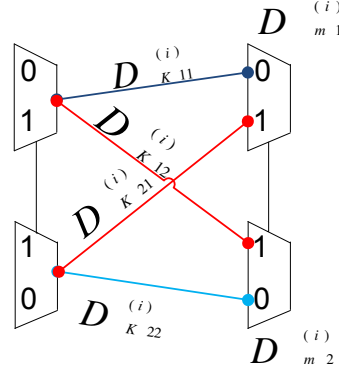


**Figure A. 1 :** Two successive MUX blocks with delay variables

Let's try to express  $u_i$  variable defined in section (3.5) in terms wire delays  $D_{K11}^{(i)}$ ,  $D_{K12}^{(i)}$ ,  $D_{K21}^{(i)}$ ,  $D_{K22}^{(i)}$  and upper MUX and lower MUX gate delays which are  $D_{m1}^{(i)}$ , and  $D_{m2}^{(i)}$ , respectively. We can achieve it by simple substitution of  $a_i, d_i, b_i, f_i$  parameters in terms of wire and gate delays which are shown in Figure A.1 .

$$a_i = D_{K11}^{(i)} + D_{m1}^{(i)} \quad (\text{A.1})$$

$$b_i = D_{K12}^{(i)} + D_{m2}^{(i)} \quad (\text{A.2})$$

$$f_i = D_{K22}^{(i)} + D_{m2}^{(i)} \quad (\text{A.3})$$

$$d_i = D_{K21}^{(i)} + D_{m1}^{(i)} \quad (\text{A.4})$$

$$\mathbf{u}_i = \frac{(a_i - d_i) + (b_i - f_i)}{2} = \frac{(D_{K11}^{(i)} + D_{m1}^{(i)} - D_{K21}^{(i)} - D_{m1}^{(i)}) + (D_{K12}^{(i)} + D_{m2}^{(i)} - D_{K22}^{(i)} - D_{m2}^{(i)})}{2} =$$

$$\frac{(D_{K11}^{(i)} - D_{K22}^{(i)}) + (D_{K12}^{(i)} - D_{K21}^{(i)})}{2} \quad (\text{A.5})$$

$$\vartheta_i = \frac{(a_i + d_i) - (b_i + f_i)}{2} = \frac{(D_{K11}^{(i)} + D_{m1}^{(i)} + D_{K21}^{(i)} + D_{m1}^{(i)}) - (D_{K12}^{(i)} + D_{m2}^{(i)} + D_{K22}^{(i)} + D_{m2}^{(i)})}{2} =$$

$$\frac{(D_{K11}^{(i)} - D_{K22}^{(i)}) + (D_{K21}^{(i)} - D_{K12}^{(i)})}{2} + (D_{m1}^{(i)} - D_{m2}^{(i)}) \quad (\text{A.6})$$

## **CURRICULUM VITAE**



**Candidate's full name** : Zaur TARIGULIYEV

**Place and Date of Birth** : Baku / AZERBAIJAN, 07.05.1979

**Permanent Address** : M.Hadi str, 23/136, Baku/ AZERBAIJAN

**Universities and**

**Colleges attended** :Istanbul Technical University (1998-2002)